In vivo discovery of immunotherapy targets in the tumour microenvironment

Citation: Zhou, Penghui, Donald R. Shaffer, Diana A. Alvarez Arias, Yukoh Nakazaki, Wouter Pos, Alexis J. Torres, Viviana Cremasco, et al. "In Vivo Discovery of Immunotherapy Targets in the Tumour Microenvironment." Nature 506, no. 7486 (January 29, 2014): 52–57.

As Published: http://dx.doi.org/10.1038/nature12988

Publisher: Nature Publishing Group

Persistent URL: http://hdl.handle.net/1721.1/89162

Version: Original manuscript: author's manuscript prior to formal peer review

In vivo Discovery of Immunotherapy Targets in the Tumor Microenvironment

Penghui Zhou,[1*] Donald R. Shaffer,[1*] Diana A. Alvarez Arias,[1] Yukoh Nakazaki,[1] Wouter Pos,[1] Alexis J. Torres,[2] Viviana Cremasco,[1] Stephanie K. Dougan,[3] Glenn S. Cowley,[4] Kutlu Elpek,[1] Jennifer Brogdon,[5] John Lamb,[6] Shannon Turley,[1] Hidde L. Ploegh,[3] David E. Root,[4] J. Christopher Love,[2] Glenn Dranoff,[1] Nir Hacohen,[4] Harvey Cantor,[1] Kai W. Wucherpfennig[1]

[1]Dana-Farber Cancer Institute, Boston, MA 02115, [2]David H. Koch Institute for Integrative Cancer Research, Massachusetts Institute of Technology, Cambridge, MA 02142, [3]Whitehead Institute, Massachusetts Institute of Technology, Cambridge, MA 02142, [4]Broad Institute of MIT and Harvard, Cambridge, MA 02142, [5]Novartis Institutes for Biomedical Research, Cambridge, MA 02139, [6]Genomics Institute of the Novartis Research Foundation, San Diego CA 92121

*These authors contributed equally

Correspondence: kai_wucherpfennig@dfci.harvard.edu

Word count for main body: 2,186

Recent work has shown that cytotoxic T cells play a central role in immune-mediated control of cancers[1-3], and monoclonal antibodies that target inhibitory receptors on T cells can induce significant clinical benefit in patients despite advanced disease[4-6]. However, many of the regulatory pathways that result in loss of T cell function within immunosuppressive tumors remain unknown. Here we show that such regulatory mechanisms can be systematically discovered *in vivo* in the tumor microenvironment. We devised a pool shRNA screening approach aimed at identifying genes that block the function of tumor-infiltrating CD8 T cells. We postulated that shRNAs targeting key inhibitors would enable robust T cell infiltration and proliferation in tumors, despite multiple inhibitory signals. Candidate shRNAs were discovered by transfer of shRNA-transduced T cells into tumor-bearing mice, followed by deep sequencing to quantify the representation of all hairpins in tumors and lymphoid organs. A subset of shRNAs induced T cell accumulation in tumors but not the spleen, demonstrating feasibility of discovering shRNAs with differential action across tissues. One of the targets was Ppp2r2d, a regulatory subunit of the family of PP2A phosphatases[7]. Control shRNA-transduced T cells underwent apoptosis upon recognition of melanoma cells, while Ppp2r2d shRNA-transduced T cells accumulated in tumors due to enhanced proliferation and reduced apoptosis. Ppp2r2d shRNA-expressing T cells also significantly delayed tumor growth. This *in vivo* approach has wide applications to dissect complex immune functions in relevant tissue microenvironments.

Immune cells perform complex surveillance functions throughout the body and interact with many different types of cells in distinct tissue microenvironments. Therapeutic targets for modulating immune responses are typically identified *in vitro* and tested in animal models at a late stage of the process. We postulate that the complex interactions of immune cells within tissues - many of which do not occur *in vitro* - offer untapped opportunities for therapeutic intervention. Here we have addressed the challenge of how targets for immune modulation can be systematically discovered *in vivo*. This is a central issue in oncology because strong infiltration by CD8 T cells - which have cytotoxic function against tumor cells - is associated with a favorable prognosis in multiple types of human cancer[1,3,8]. Unfortunately, this natural defense mechanism is severely blunted in the majority of patients by multiple inhibitory signals emanating from the tumor, its stroma, regulatory T cells and myeloid cell populations.[9-11]

Pooled shRNA libraries have been shown to be powerful discovery tools[12,13]. We reasoned that shRNAs capable of restoring CD8 T cell function can be systematically discovered *in vivo* by taking advantage of the extensive proliferative capacity of T cells following triggering of the T cell receptor by a tumor-associated antigen. When introduced into T cells, only a small subset of shRNAs from a pool will restore T cell proliferation resulting in their enrichment within tumors. Over-representation of active shRNAs within each pool can be quantified by deep sequencing of the shRNA cassette from tumors and secondary lymphoid organs (Fig. 1a).

We chose B16 melanoma, an aggressive tumor that is difficult to treat[14]. Melanoma cells expressed the surrogate tumor antigen Ovalbumin (Ova), which is recognized by CD8 T cells from OT-I T cell receptor transgenic mice[15,16]. Initial experiments showed that such a screen could also be performed with pmel-1 T cells that recognize gp100, an endogenous melanoma antigen[17], but the signal/noise ratio was lower for pmel-1 T cells due to smaller T cell populations in tumors. Naïve T cells are difficult to infect with lentiviral vectors, and we therefore pretreated T cells for two days with the homeostatic

cytokines IL-7 and IL-15 prior to spin infection with shRNA pools in a lentiviral vector. Successful transduction was monitored by surface expression of the Thy1.1 reporter (Fig. S1a). T cells were injected into B6 mice bearing day 14 B16-Ova tumors. Seven days later, T cells were purified from tumors and secondary lymphoid organs (spleen, tumor-draining and irrelevant lymph nodes) for isolation of genomic DNA, followed by PCR amplification of the shRNA cassette (Fig. S1b). The representation of shRNAs was then quantified in different tissues by Illumina sequencing.

Two large screens were performed, with the first focusing on genes over-expressed in dysfunctional T cells (T cell anergy or exhaustion; 255 genes, 1,275 shRNAs divided into two pools), and the second on kinases/phosphatases (1,307 genes, 6,535 shRNAs divided into seven pools) (Fig. 1b). In these primary screens, each gene was represented by ~5 shRNAs (it is common that only one or two of such shRNAs have sufficient activity in pooled screens). We observed multiple distinct *in vivo* phenotypes. For certain genes, shRNAs were over-represented in all tested tissues compared to the starting T cell population (e.g. SHP-1), indicative of enhanced proliferation independent of T cell receptor recognition of a tumor antigen. For other genes, there was a selective loss of shRNAs within tumors (e.g. ZAP-70, a critical kinase in the T cell activation pathway). We focused our analysis on genes whose shRNAs showed substantial over-representation in tumor but not spleen, a secondary lymphoid organ. Substantial T cell accumulation in tumors was observed for a number of shRNAs, despite the immunosuppressive environment. For secondary screens, we created focused pools in which each candidate gene was represented by ~15 shRNAs. Primary data from this analysis are shown for three genes in Fig. 1c: LacZ (negative control), Cblb (an E3 ubiquitin ligase that induces T cell receptor internalization)[18] and Ppp2r2d (not previously studied in T cells). For both Ppp2r2d and Cblb, five shRNAs were substantially increased in tumors (red) compared to spleen, while no enrichment was observed for LacZ shRNAs. Overall, 43 genes met the following criteria: ≥4-fold enrichment for 3 or

more shRNAs in tumors compared to spleen (Fig. 1b, Fig. S1c,d). The set included gene products previously identified as inhibitors of T cell receptor signaling (including Cblb, Dgka, Dgkz, Ptpn2) as well as other well-known inhibitors of T cell function (e.g. Smad2, Socs1, Socs3, Egr2), validating our approach (Fig. 1d, Fig. S2).[19-21]

We next confirmed at a cellular level that these shRNAs induce T cell accumulation in tumors. T cells were infected with lentiviral vectors driving expression of a single shRNA and a reporter protein (Thy1.1 or one of four different fluorescent proteins), and after seven days the frequency of shRNA-transduced T cells was quantified in tumors, spleens and lymph nodes by flow cytometry. When the control LacZ shRNA was expressed in CD8 T cells, the frequency of shRNA-expressing CD8 T cells was lower in tumors compared to spleen (~2-fold). In contrast, experimental shRNAs induced accumulation of CD8 T cells in tumors but not the spleen (Fig. 2a, Fig. S3). For seven of these genes, T cell accumulation in tumors was >10-fold relative to spleen. The strongest phenotype was observed with shRNAs targeting Ppp2r2d, a regulatory subunit of the family of PP2A phosphatases[7]. A Ppp2r2d shRNA not only induced accumulation of OT-I CD8 T cells, but also CD4 T cells (from TRP-1 TCR transgenic mice)[22], with T cell numbers in tumors being significantly higher when Ppp2r2d rather than LacZ shRNA was expressed (36.3-fold for CD8; 16.2-fold for CD4 T cells) (Fig. 2b). CD8 T cell accumulation correlated with the degree of Ppp2r2d knock-down, and two Ppp2r2d shRNAs with the highest *in vivo* activity induced the lowest levels of Ppp2r2d mRNA (Fig. S3b). Ppp2r2d knockdown was also confirmed at the protein level using a quantitative mass spectrometry approach (Fig. S3c). Ppp2r2d shRNA activity was specific because the phenotype was reversed when a Ppp2r2d cDNA (with wild-type protein sequence, but mutated DNA sequence at the shRNA binding site) was co-introduced with the Ppp2r2d shRNA (Fig. 2c, Fig. S4). Furthermore, OT-I CD8 T cells over-expressed Ppp2r2d in tumors compared to spleen (in the absence of any shRNA expression), suggesting that it is an intrinsic

component of the signaling network inhibiting T cell function in tumors (Fig. 2d). Microarray analysis of tumor-infiltrating T cells expressing different shRNAs showed that each shRNA induced a largely distinct set of gene expression changes, indicating that improved T cell function in tumors can be mediated through a number of different intracellular pathways (Fig. S5).

We next examined the cellular mechanisms driving T cell accumulation by a Ppp2r2d shRNA in tumors - specifically T cell infiltration, proliferation and apoptosis. T cell infiltration into tumors was assessed by transfer of OT-I CD8 T cells labeled with a cytosolic dye, CFSE. No differences were observed in the frequency of Ppp2r2d or LacZ shRNA-transduced CD8 T cells in tumors on day 1, arguing against a substantial effect on T cell infiltration (Fig. 3a). However, analysis of later time points (days 3-7) demonstrated a higher degree of proliferation (based on CFSE dilution) by Ppp2r2d compared to LacZ shRNA-transduced T cells (Fig. 3b, Fig. S6a). Substantial T cell proliferation was even observed for LacZ shRNA-transduced T cells (complete dilution of CFSE dye by day 7), despite the presence of small numbers of such cells in tumors. This suggested that LacZ shRNA-transduced T cells were lost by apoptosis. Indeed, a larger percentage of tumor-infiltrating T cells were labeled with an antibody specific for active caspase-3 when the LacZ control shRNA (rather than Ppp2r2d shRNA) was expressed (Fig. 3c, Fig. S6b). Furthermore, co-culture of CD8 T cells with B16-Ova tumor cells showed that the majority of LacZ shRNA expressing T cells became apoptotic (65.7%) while the majority of Ppp2r2d shRNA-transduced T cells were viable (89.5%, Fig. S6c). *Ex vivo* analysis of tumor-infiltrating T cells at a single-cell level with a nanowell device also demonstrated increased cytokine production by T cells expressing Ppp2r2d compared to LacZ shRNA (Fig. S7b, c). In addition, intracellular cytokine staining confirmed production of higher levels of interferon-γ (IFNγ), a cytokine critical for anti-tumor immunity (Fig. 3d, S7a). The action of Ppp2r2d was downstream of T cell receptor activation because T cell proliferation was enhanced in tumors and to a lesser extent in tumor-draining lymph nodes (Fig. S6). In

contrast, no proliferation was observed in irrelevant lymph nodes or the spleen where the relevant antigen is not presented to T cells (data not shown).

These results suggested the possibility that Ppp2r2d shRNA-transduced CD8 T cells may be able to proliferate and survive even when they recognize their antigen directly presented by B16-Ova tumor cells. This idea was tested by implantation of tumor cells into *b2m-/-* mice which are deficient in expression of MHC class I proteins[23]. In such mice, only tumor cells but not professional antigen presenting cells of the host could present tumor antigens to T cells. Indeed, Ppp2r2d shRNA-transduced OT-I CD8 T cells showed massive accumulation within B16-Ova tumors in *b2m-/-* mice (Fig. 3e) while there were very small numbers of T cells in contralateral B16 tumors that lacked expression of the Ova antigen. T cells expressing a Ppp2r2d shRNA could thus effectively proliferate and survive in response to tumor cells, despite a lack of suitable co-stimulatory signals and an inhibitory microenvironment.

PP2A represents a family of phosphatase complexes composed of catalytic, scaffolding and regulatory subunits. Cellular localization and substrate specificity are determined by one of many regulatory subunits of which Ppp2r2d is a member[7]. Ppp2r2d directs PP2A to Cdk1 substrates during interphase and anaphase; it thereby inhibits entry into mitosis and induces exit from mitosis[24]. PP2A also plays a gatekeeper role for BAD-mediated apoptosis. Phosphorylated BAD is sequestered in its inactive form in the cytosol by 14-3-3, while dephosphorylated BAD is targeted to mitochondria where it causes cell death by binding Bcl-X_L and Bcl-2[25]. PP2A phosphatases have also been shown to interact with the cytoplasmic domains of CD28 and CTLA-4 as well as Carma1 (upstream of the NF-κB pathway)[26,27], but it is not known which regulatory subunits are required for these activities; Ppp2r2d antibodies suitable for the required biochemical studies are currently not available.

Finally, we assessed the ability of a Ppp2r2d shRNA to enhance the efficacy of adoptive T cell therapy. B16-Ova tumor cells ($2x10^5$) were injected subcutaneously into B6 mice. On day 12, mice bearing tumors of similar size were divided into seven groups, either receiving no T cells, $2x10^6$ shRNA-transduced TRP-1 CD4 T cells, $2x10^6$ shRNA infected OT-I CD8 T cells, or both CD4 and CD8 T cells (days 12 and day 17). The modest anti-tumor activity of OT-I CD8 T cells (expressing the control LacZ shRNA) is consistent with published data[28]. Ppp2r2d shRNA improved the therapeutic activity of both CD4 and CD8 T cells (Fig. 4a,b). A Ppp2r2d shRNA also enhanced anti-tumor responses when introduced into T cells specific for the endogenous melanoma antigens gp100 (pmel-1 CD8 T cells) and TRP-1 (TRP-1 CD4 T cells) (Fig. 4c). Gp100 is a relevant antigen in human melanoma, and a clinical trial in which a gp100-specific TCR (isolated from HLA-A2 transgenic mice) was introduced into peripheral blood T cells demonstrated therapeutic benefit in a subset of patients [29].

T cells expressing Ppp2r2d shRNAs acquired an effector phenotype in tumors (Fig. S8a) and >30% of the cells expressed granzyme B (Fig. S8c). Consistent with greatly increased numbers of such effector T cells in tumors (Fig. S9a), TUNEL staining demonstrated increased apoptosis in tumors when Ppp2r2d rather than LacZ shRNA expressing T cells were present (Fig. S9b). B16 melanomas are highly aggressive tumors in part because MHC class I expression is very low. Interestingly, Ppp2r2d but not LacZ shRNA-expressing T cells significantly increased MHC class I expression ($H\text{-}2K^b$) by tumor cells, possibly due to the observed increase in IFNγ secretion by T cells (Fig. S9c, Fig. S7). A Ppp2r2d shRNA did not reduce expression of inhibitory PD-1 or LAG-3 receptors on tumor-infiltrating T cells, demonstrating that its mechanism of action is distinct from these known negative regulators of T cell function (Fig. S8b). This finding suggests combination approaches targeting these intracellular and cell surface molecules.

These results establish the feasibility of *in vivo* discovery of novel targets for immunotherapy in complex tissue microenvironments. We show that it is possible to discover genes with differential action across tissues, as exemplified by T cell accumulation in tumors compared to secondary lymphoid organs. For genes with tissue-selective action, T cell proliferation and survival are likely to be under the control of the T cell receptor and therefore do not occur in tissues lacking presentation of a relevant antigen. Targeting of such genes may offer new approaches to modify the activity of T cells in cancer and other pathologies. For example, recent clinical trials have shown that transfer of genetically modified T cells can result in substantial anti-tumor activity[30]. The efficacy of such T cell therapies could be enhanced by shRNA-mediated targeting of genes that inhibit T cell function in the tumor microenvironment.

Methods Summary

***In vivo* shRNA screening.** Nine shRNA pools (~5 shRNAs per gene) were created and subcloned into the pLKO-Thy1.1 lentiviral vector. Each pool also included 85 negative-control shRNAs. OT-I T cells were cultured with IL-7 (5ng/mL) and IL-15 (100ng/mL); on day 2 cells were spin-infected with lentiviral pools supplemented with protamine sulfate (5μg/mL) in retronectin-coated 24-well plates (5μg/mL) at a multiplicity of infection (MOI) of 15. Following infection, OT-1 cells were cultured with IL-7 (2.5ng/mL), IL-15 (50ng/mL) and IL-2 (2ng/mL). On day 5, shRNA-transduced T cells were enriched by positive selection using the Thy1.1 surface reporter (Stemcell Technologies). T cells (5×10^6) were injected i.v. into C57BL/6 mice bearing day 14 B16-Ova tumors (15 mice per shRNA pool). Seven days later, shRNA-expressing T cells ($CD8^+V\alpha2^+V\beta5^+Thy1.1^+$) were isolated by flow cytometry from tumors, spleens, tumor-draining lymph nodes and irrelevant lymph nodes. Genomic DNA was purified (Qiagen) and deep-sequencing templates were generated by PCR amplification of the shRNA cassette. Representation of shRNAs in each pool was analyzed by deep sequencing using an Illumina Genome Analyzer[31].

Secondary screens were performed using focused pools containing ~15 shRNAs/gene as well as 85 negative controls. Cut-off in the secondary screen was defined as $\geq$3 shRNAs with $\geq$4 fold enrichment in tumor relative to spleen. Screening results were validated at a cellular level by introducing individual shRNAs into T cells, along with a reporter protein (GFP, TFP, RFP or Ametrine fluorescent proteins, Thy1.1). This approach enabled simultaneous testing of five shRNAs in an animal (three mice per group). Proliferation of shRNA-transduced T cells was visualized based on CFSE dilution after 24 hours as well as 3, 5 and 7 days.

31. Ashton, J.M.*, et al.* Gene sets identified with oncogene cooperativity analysis regulate in vivo growth and survival of leukemia stem cells. *Cell Stem Cell* **11**, 359-372 (2012).

References

1. Galon, J., *et al.* Type, density, and location of immune cells within human colorectal tumors predict clinical outcome. *Science* **313**, 1960-1964 (2006).
2. Hamanishi, J., *et al.* Programmed cell death 1 ligand 1 and tumor-infiltrating CD8+ T lymphocytes are prognostic factors of human ovarian cancer. *Proceedings of the National Academy of Sciences of the United States of America* **104**, 3360-3365 (2007).
3. Mahmoud, S.M., *et al.* Tumor-Infiltrating CD8+ Lymphocytes Predict Clinical Outcome in Breast Cancer. *J Clin Oncol* **29**, 1949-1955 (2011).
4. Topalian, S.L., *et al.* Safety, activity, and immune correlates of anti-PD-1 antibody in cancer. *The New England journal of medicine* **366**, 2443-2454 (2012).
5. Brahmer, J.R., *et al.* Safety and activity of anti-PD-L1 antibody in patients with advanced cancer. *The New England journal of medicine* **366**, 2455-2465 (2012).
6. Hodi, F.S., *et al.* Improved Survival with Ipilimumab in Patients with Metastatic Melanoma. *N Engl J Med* (2011).
7. Barr, F.A., Elliott, P.R. & Gruneberg, U. Protein phosphatases and the regulation of mitosis. *J Cell Sci* **124**, 2323-2334 (2011).
8. Pages, F., *et al.* In situ cytotoxic and memory T cells predict outcome in patients with early-stage colorectal cancer. *J Clin Oncol* **27**, 5944-5951 (2009).
9. Shiao, S.L., Ganesan, A.P., Rugo, H.S. & Coussens, L.M. Immune microenvironments in solid tumors: new targets for therapy. *Genes Dev* **25**, 2559-2572 (2011).
10. Gabrilovich, D.I. & Nagaraj, S. Myeloid-derived suppressor cells as regulators of the immune system. *Nat Rev Immunol* **9**, 162-174 (2009).
11. Topalian, S.L., Drake, C.G. & Pardoll, D.M. Targeting the PD-1/B7-H1(PD-L1) pathway to activate anti-tumor immunity. *Current opinion in immunology* **24**, 207-212 (2012).
12. Westbrook, T.F., *et al.* A genetic screen for candidate tumor suppressors identifies REST. *Cell* **121**, 837-848 (2005).
13. Zender, L., *et al.* An oncogenomics-based in vivo RNAi screen identifies tumor suppressors in liver cancer. *Cell* **135**, 852-864 (2008).
14. Fidler, I.J. Biological behavior of malignant melanoma cells correlated to their survival in vivo. *Cancer research* **35**, 218-224 (1975).
15. Hogquist, K.A., *et al.* T cell receptor antagonist peptides induce positive selection. *Cell* **76**, 17-27 (1994).
16. Bellone, M., *et al.* Relevance of the tumor antigen in the validation of three vaccination strategies for melanoma. *Journal of immunology* **165**, 2651-2656 (2000).
17. Overwijk, W.W., *et al.* Tumor regression and autoimmunity after reversal of a functionally tolerant state of self-reactive CD8+ T cells. *The Journal of experimental medicine* **198**, 569-580 (2003).
18. Paolino, M. & Penninger, J.M. Cbl-b in T-cell activation. *Semin Immunopathol* **32**, 137-148 (2010).
19. Zheng, Y., Zha, Y. & Gajewski, T.F. Molecular regulation of T-cell anergy. *EMBO Rep* **9**, 50-55 (2008).
20. Doody, K.M., Bourdeau, A. & Tremblay, M.L. T-cell protein tyrosine phosphatase is a key regulator in immune cell signaling: lessons from the knockout mouse model and implications in human disease. *Immunological reviews* **228**, 325-341 (2009).
21. Tamiya, T., Kashiwagi, I., Takahashi, R., Yasukawa, H. & Yoshimura, A. Suppressors of cytokine signaling (SOCS) proteins and JAK/STAT pathways: regulation of T-cell inflammation by SOCS1 and SOCS3. *Arterioscler Thromb Vasc Biol* **31**, 980-985 (2011).
22. Muranski, P., *et al.* Tumor-specific Th17-polarized cells eradicate large established melanoma. *Blood* **112**, 362-373 (2008).
23. Koller, B.H., Marrack, P., Kappler, J.W. & Smithies, O. Normal development of mice deficient in beta 2M, MHC class I proteins, and CD8+ T cells. *Science* **248**, 1227-1230 (1990).
24. Mochida, S., Maslen, S.L., Skehel, M. & Hunt, T. Greatwall phosphorylates an inhibitor of protein phosphatase 2A that is essential for mitosis. *Science* **330**, 1670-1673 (2010).

25. Chiang, C.W.*, et al.* Protein phosphatase 2A dephosphorylation of phosphoserine 112 plays the gatekeeper role for BAD-mediated apoptosis. *Mol Cell Biol* **23**, 6350-6362 (2003).
26. Chuang, E.*, et al.* The CD28 and CTLA-4 receptors associate with the serine/threonine phosphatase PP2A. *Immunity* **13**, 313-322 (2000).
27. Eitelhuber, A.C.*, et al.* Dephosphorylation of Carma1 by PP2A negatively regulates T-cell activation. *Embo J* **30**, 594-605 (2011).
28. Tao, J.*, et al.* JNK2 negatively regulates CD8+ T cell effector function and anti-tumor immune response. *Eur J Immunol* **37**, 818-829 (2007).
29. Johnson, L.A.*, et al.* Gene therapy with human and mouse T-cell receptors mediates cancer regression and targets normal tissues expressing cognate antigen. *Blood* **114**, 535-546 (2009).
30. Turtle, C.J., Hudecek, M., Jensen, M.C. & Riddell, S.R. Engineered T cells for anti-cancer therapy. *Current opinion in immunology* **24**, 633-639 (2012).

Supplementary information is linked to the online version of the paper at www.nature.com/nature.

Acknowledgements

This work was supported by the National Institutes of Health (Transformative Research Award 1R01CA173750 to K.W.W.), the Melanoma Research Alliance (to K.W.W.), the DF/HCC – MIT Bridge Project and the Lustgarten Foundation (to K.W.W., J.C.L. and H.P.), Novartis Institutes of Biomedical Research (to K.W.W.), the Koch Institute Support Grant P30-CA14051 from the National Cancer Institute, the American Cancer Society John W. Thatcher, Jr. Postdoctoral Fellowship in Melanoma Research (to D.S.), the Terri Brodeur Breast Cancer Foundation Postdoctoral Fellowship (to P.Z.) and a NIH T32 grant (AI07386 to D.A.A.A.).

Author information

Contributions

K.W.W., P.Z. and D.S. designed experiments; P.Z., D.A.A.A. and H.C. developed procedure for lentiviral infection of T cells and optimized approaches for adoptive T cell therapy; P.Z., D.S. and D.A.A.A. performed shRNA screen; G.S.C., D.E.R. and N.H. provided pooled shRNA library and advice on shRNA screen; Y.N. and G.D. provided B16-Ova cell line and advice on tumor model; A.J.T. and J.C.L. performed nanowell analysis of cytokine production, V.C. and S.T. performed histological studies, W.P. performed protein quantification by mass spectrometry, S.K.D. and H.L.P. provided

mouse models; J.B., K.E. and J.L. performed microarray analysis; K.W.W., P.Z. and D.S. wrote the paper.

Competing financial interests

K.W.W. and G.D. served as consultants to Novartis.

Correspondence and requests for materials should be addressed to kai_wucherpfennig@dfci.harvard.edu.

Figure legends

Figure 1 □ *In vivo* RNAi discovery of immunotherapy targets. **a**, Approach for *in vivo* discovery of shRNAs that enhance T cell function in tumors. OT-I CD8 T cells cultured in IL-7/IL-15 were transduced with shRNA pools and injected into mice bearing day 14 B16-Ova tumors. Seven days later, OT-I T cells were isolated from tumors and lymphoid organs. The shRNA cassette was amplified by PCR using genomic DNA from purified T cells. Representation of all hairpins was quantified in different organs by deep sequencing. **b**, Summary of shRNA screens for kinases/phosphatases and genes upregulated in dysfunctional T cells. Positive genes in secondary screen were defined as $\underline{\geq}3$ shRNAs with $\geq$4-fold enrichment in tumors relative to spleen. **c**, Deep sequencing data from *in vivo* shRNA pool screen. Upper row, sequence reads for all genes in a pool in tumor, irrelevant (irLN) and draining lymph node (dLN); lower row, three individual genes (LacZ, negative control). Sequence reads are plotted for these tissues versus spleen. Dashed lines indicate a deviation by $\log_2$ from diagonal. **d**, Functional classification of candidate genes from secondary screen.

Figure 2 □ shRNA-driven accumulation of CD4 and CD8 T cells in B16 melanoma. **a**, Flow cytometry-based quantification of CD8 T cell enrichment in tumors. OT-I T cells transduced with lentiviral shRNA vectors were injected into mice bearing day 14 B16-Ova tumors. Seven days later, percentage of shRNA-expressing T cells was determined by flow cytometry in tumors/spleens by gating on reporter proteins in $CD8^+V\alpha2^+V\beta5^+$ T cells. Statistical significance was determined for each experimental shRNA against LacZ shRNA (fold enrichment tumor/spleen) (n=3). **b**, $CD8^+$ OT-I or $CD4^+$ TRP-1 T cells expressing Ppp2r2d or LacZ shRNAs were injected into mice bearing day 14 B16-

Ova tumors. Thy1.1 reporter was used to identify shRNA-expressing T cells in tumors and spleens (% Thy1.1$^+$ CD8 T cells, left panels). Total numbers of LacZ or Ppp2r2d shRNA-expressing T cells were determined in tumors and spleens 7 days following transfer of 2x10^6 shRNA-expressing cells (right panels). Fold-enrichment of Ppp2r2d versus LacZ shRNA-expressing T cells in tumors is indicated (n=4). **c**, Reversal of Ppp2r2d shRNA-mediated T cell expansion in tumors by Ppp2r2d cDNA with wild-type protein sequence but mutated shRNA binding site. OT-I T cells transduced with lentiviral vectors driving expression of LacZ shRNA, Ppp2r2d shRNA, or Ppp2r2d shRNA + Ppp2r2d mutant cDNA were co-injected into B16-Ova bearing mice (n=4). The three cell populations were identified based on co-expressed reporters; fold-enrichment was calculated based on percentage of reporter-positive cells in tumors versus spleens. **d**, qPCR quantification of Ppp2r2d mRNA levels in OT-I T cells (not expressing a shRNA) 7 days after transfer into B16-Ova tumor-bearing mice (representative data from two independent experiments). Statistical significance was determined using Student's *t*-test, * $p \leq 0.05$, ** $p \leq 0.01$; error bars denote standard deviation.

Figure 3 □ Changes in T cell function induced by Ppp2r2d shRNA. a, T cell infiltration into tumors. OT-I T cells expressing Ppp2r2d or LacZ shRNAs were labeled with CFSE and injected into B16-Ova tumor-bearing mice. Twenty-four hours later transduced T cells were isolated from tumors and spleens and quantified by flow cytometry gating on CD8+ T cells. **b**, Ppp2r2d shRNA increases T cell proliferation in tumors. Design described in (**a**) was used to assess T cell proliferation on days 1, 3, 5 and 7 based on CFSE dilution. **c**, Ppp2r2d-silencing inhibits T cell apoptosis in tumors. OT-I cells expressing Ppp2r2d or LacZ shRNAs were injected into B16-Ova tumor-bearing mice. Seven days later, transduced T cells were harvested and apoptotic cells were identified by flow cytometry following labeling with an antibody specific for activated caspase-3. **d**, Increased IFN-γ secretion by Ppp2r2d-

silenced T cells. OT-I T cells isolated from B16-Ova tumor-bearing mice were assayed for IFN-γ expression by intracellular staining. **e**, Ppp2r2d-silenced T cells expand in tumors even without presentation of tumor antigens by professional antigen presenting cells. LacZ or Ppp2r2d shRNA-expressing OT-I T cells were transferred into day 14 B16-Ova tumor-bearing C57BL/6 or *b2m-/-* mice. shRNA-expressing T cells were identified based on expression of teal fluorescent protein (TFP) or Thy1.1 (fold enrichment in tumors compared to spleens). For all experiments data representative of two independent trials (n=3; ** $p \leq 0.01$, Student's *t*-test); error bars denote standard deviation.

Figure 4 □ Silencing of Ppp2r2d enhances anti-tumor activity of CD4 and CD8 T cells. T cells were activated with anti-CD3/CD28 beads, infected with lentiviruses driving LacZ or Ppp2r2d shRNA expression and injected into B16-Ova (**a,b**) or B16 (**c**) tumor-bearing mice. Tumor size was measured every three days following T cell transfer using calipers on the two longest axes. **a,b** $CD4^+$ TRP-1 and/or $CD8^+$ OT-I T cells (2×10^6) were transferred (day 12 and 17) into mice bearing day 12 B16-Ova tumors. Tumor burden (**a**) and survival (**b**) were assessed. **c**, $CD4^+$ TRP-1 and $CD8^+$ pmel-1 T cells ($3x10^6$ $CD4^+$ TRP-1 plus $3x10^6$ $CD8^+$ pmel-1) were transferred (day 10 and 15) into mice with day 10 B16 tumors. Log-rank (Mantel-Cox) test was performed using GraphPad Prism version 6 comparing survival of mice treated with LacZ versus Ppp2r2d shRNA-expressing T cells. Error bars denote standard error of the mean. Data representative of two independent experiments (n=7-9 mice/group).

Methods

***In vivo* shRNA screening.** shRNAs targeting 255 genes over-expressed in dysfunctional T cells (anergic or exhausted state)[32-38] and 1,307 kinase/phosphatase genes (~5 shRNAs per gene) were obtained from The RNAi Consortium (TRC; Broad Institute, Cambridge, MA, USA). Nine pools were created and shRNAs subcloned into the pLKO-Thy1.1 lentiviral vector. Each pool also contained 85 negative-control shRNAs (number of shRNAs: GFP, 24; LacZ, 20; luciferase 25; RFP 16). OT-I T cells isolated by negative selection (Stemcell Technologies) were cultured with IL-7 (5ng/mL, Peprotech) and IL-15 (100ng/mL, Peprotech) in complete RPMI media (RPMI 1640, 10% FBS, 20mM HEPES, 1mM sodium pyruvate, 0.05mM 2-mercaptoethanol, 2mM L-glutamine, 100μg/ml streptomycin and 100μg/ml penicillin). On day 2, OT-I T cells ($2x10^6$/well) were spin-infected with lentiviral pools supplemented with protamine sulfate (5 μg/mL) in 24-well plates coated with retronectin (5μg/mL) at a multiplicity of infection (MOI) of 15. Typically ~$50x10^6$ OT-1 T cells were infected for each pool. Following infection, OT-I cells were cultured with IL-7 (2.5ng/mL), IL-15 (50ng/mL) and IL-2 (2ng/mL, BioLegend) in complete RPMI media. On day 5, live cells were enriched using a dead cell removal kit (Miltenyi), and infected cells (20-25% Thy1.1+) were positively selected based on Thy1.1 marker (Stemcell Technologies) to 50-60% Thy1.1 positivity. T cells (5×10^6) were injected i.v. into C57BL/6 mice bearing day 14 B16-Ova tumors ($2x10^5$ tumor cells injected on day 0), 15 mice per shRNA pool. Genomic DNA was isolated from 5×10^6 enriched OT-I cells as the start population for deep sequencing. Seven days later, shRNA-expressing T cells ($CD8^+V\alpha2^+V\beta5^+Thy1.1^+$) were isolated by flow cytometry from tumors, spleens, tumor-draining lymph nodes and irrelevant lymph nodes. Genomic DNA was isolated (Qiagen) and deep-sequencing templates were generated by PCR of the shRNA cassette. Representation of shRNAs in each pool was analyzed by deep sequencing using an

Illumina Genome Analyzer[31]. Data were normalized using the average reads of control shRNAs in each pool. Kinase/phosphatase genes were selected for the secondary screen based on expression levels in T cells (Immunological Genome Project, http://www.immgen.org/). For the secondary screen, ~10 additional shRNAs were synthesized for each gene (IDT) for a total of ~15 shRNAs per gene. These focused pools contained 85 negative-control shRNAs. Two control shRNAs (one for RFP, one for luciferase) showed some enrichment in tumors relative to spleen (4.0 and 5.1-fold, respectively). Cut-off in the secondary screen was defined as $\geq$3 shRNA, with $\geq$4 fold enrichment in tumors relative to spleen.

T cell isolation from tumors. B16-Ova melanomas were cut into small pieces in petri dishes containing 5mL of PBS, 2% FBS and washed with PBS. Tumors were resuspended in 15 mL RPMI supplemented with 2% FBS, 50U/mL Collagenase Type IV (Invitrogen), 20U/mL DNase (Roche), samples incubated at 37º C for 2 hours and tissue further dissociated using a gentleMACS Dissociator (Miltenyi Biotech). Suspensions were washed three times with PBS and passed through a 70 μM strainer. Lymphocytes were isolated by density gradient centrifugation and then either analyzed or sorted by flow cytometry using a FACSAria (BD Biosciences).

Quantification of T cell enrichment in tumors by flow cytometry. Individual shRNAs were cloned into lentiviral vectors encoding five different reporter proteins (GFP, TFP, RFP or Ametrine fluorescent proteins, Thy1.1). Cytokine-pretreated OT-I T cells were transduced with lentiviral vectors driving expression of a single shRNA/reporter; 1×10^6 T cells of each population were mixed and co-injected i.v. into C57BL/6 mice bearing day 14 B16-Ova tumors. Seven days later, T cell populations were identified by flow cytometry based on co-introduced reporters. Fold-enrichment in tumors compared to spleen was calculated based on the percentage of OT-I T cells in each organ expressing a particular reporter. In other experiments, 2×10^6 OT-I CD8 or TRP-1 CD4 T cells were transduced with lentiviral

vectors encoding Ppp2r2d or LacZ shRNAs (Thy1.1 reporter) and injected into mice bearing day 14 B16-Ova (for OT-I T cells) or B16 (for TRP-1 T cells) tumors. On day 7, absolute numbers of shRNA-expressing T cells were determined in tumors and spleens.

T cell migration, proliferation and cytokine secretion. OT-I T cells expressing LacZ or Ppp2r2d shRNAs were purified using the Thy1.1 reporter and cultured in complete RPMI media without added cytokines for 24 hours. Live cells isolated by Ficoll density gradient centrifugation (Sigma) were labeled with CFSE (carboxyfluorescein diacetate, succinimidyl ester, Invitrogen), and 2×10^6 labeled cells were injected into mice bearing day 14 B16-Ova tumors. CFSE dilution was quantified by flow cytometry at 24 hours and days 3, 5 and 7 following transfer. In addition, intracellular staining was performed on days 3, 5 and 7 for IFNγ, TNFα and isotype controls (BD).

T cell apoptosis. Cytokine pre-treated OT-I cells were transduced with LacZ or Ppp2r2d shRNAs and injected into mice bearing day 14 B16-Ova tumors. After 7 days, intracellular staining was performed using an activated caspase-3 antibody (Cell Signaling) and CD8/Thy1.1 double-positive T cells were gated in the FACS analysis.

Treatment of tumors by adoptive T cell transfer. B16-Ova cells (2×10^5) were injected s.c. into female C57BL/6 mice (10 weeks of age). On day 12, mice bearing tumors of similar size were randomized into 7 groups (7-9 mice/group; sample size based on therapeutic activity of ppp2r2d OT-1 T cells in small pilot experiments). Anti-CD3/CD28 bead activated CD4 TRP-1 or/and CD8 OT-I T cells infected with Ppp2r2d or LacZ shRNA vectors ($2x10^6$ T cells each) were injected i.v. on days 12 and day 17. For the treatment of B16 tumors, mice were treated at day 10 with anti-CD3/CD28 bead activated CD4 TRP-1 and CD8 pmel-1 T cells expressing Ppp2r2d or LacZ shRNAs ($3x10^6$ T cells each). Tumor size was measured every three days following transfer and calculated as length × width

(investigator performing measurements was blinded to treatment group). Mice with tumors ≥20 mm on the longest axis were sacrificed.

32. Wherry, E.J., *et al.* Molecular signature of CD8+ T cell exhaustion during chronic viral infection. *Immunity* **27**, 670-684 (2007).
33. Parish, I.A., *et al.* The molecular signature of CD8+ T cells undergoing deletional tolerance. *Blood* **113**, 4575-4585 (2009).
34. Macian, F., *et al.* Transcriptional mechanisms underlying lymphocyte tolerance. *Cell* **109**, 719-731 (2002).
35. Zha, Y., *et al.* T cell anergy is reversed by active Ras and is regulated by diacylglycerol kinase-alpha. *Nat Immunol* **7**, 1166-1173 (2006).
36. Lopes, A.R., *et al.* Bim-mediated deletion of antigen-specific CD8 T cells in patients unable to control HBV infection. *The Journal of clinical investigation* **118**, 1835-1845 (2008).
37. Kurella, S., *et al.* Transcriptional modulation of TCR, Notch and Wnt signaling pathways in SEB-anergized CD4+ T cells. *Genes Immun* **6**, 596-608 (2005).
38. Xu, T., *et al.* Microarray analysis reveals differences in gene expression of circulating CD8(+) T cells in melanoma patients and healthy donors. *Cancer research* **64**, 3661-3667 (2004).

Supplementary Figure 1 □ *In vivo* RNAi screening procedure. a, Infection of $CD8^+$ T cells from $Rag1^{-/-}$/OT-I TCR transgenic mice with shRNA pools. T cells were either activated with anti-CD3/CD28 beads or exposed to recombinant murine IL-7/IL-15 for 48 hours. T cells were then infected with a LacZ control shRNA lentiviral vector and cultured for an additional three days. Transduction efficiency was determined based on expression of the Thy1.1 reporter encoded by the lentiviral vector. Cytokine-cultured T cells expressing the LacZ control shRNA were then stained with a panel of activation markers (blue lines; isotype control, shaded). The majority of infected T cells exhibited a central memory phenotype ($CD62L^+CD44^+$). **b**, Representative flow cytometry plots of OT-I T cells sorted from tumors and secondary lymphoid organs for deep sequencing analysis (dLN, tumor-draining lymph node; irLN, irrelevant lymph node). $CD8^+V\alpha2^+V\beta5^+Thy1.1^+$ cells were sorted and genomic DNA was extracted for PCR amplification of the shRNA cassette. **c**, Deep sequencing results from T cell dysfunction screen. shRNA sequencing reads for genes positive in secondary screen are plotted in comparison to spleen for tumors (red), irrelevant lymph nodes (irLN, blue) and tumor-draining lymph nodes (dLN, green), with dashed lines indicating a deviation of $\log_2$ from the diagonal. Data show enrichment of particular shRNAs representing these genes in tumors compared to spleens or lymph nodes. **d**, Deep sequencing results from kinase and phosphatase screen, as described in (**c**).

Supplementary Figure 2 □ Tumor-enriched shRNAs from secondary screen. Secondary screens were performed with a total of ~15 shRNAs for each gene of interest. **a**, Results from secondary screen of T cell dysfunction pool shRNA library. Genes for which at least 3 shRNAs showed $\geq$4 fold enrichment in tumors are listed, along with a brief description of their function. **b**, Results from secondary screen of kinase and phosphatase shRNA libraries.

Supplementary Figure 3 □ Validation of shRNAs from *in vivo* RNAi screen. a, FACS-based analysis of T cell enrichment in tumors. Positive shRNAs from deep sequencing analysis were cloned into vectors driving expression of one of four distinct fluorescent proteins (TFP, GFP, RFP, Ametrine) or Thy1.1. OT-I T cells were transduced with shRNA vectors and the five populations of T cells (normalized for transduction efficiency) were co-injected into B16-Ova tumor-bearing mice. T cells were isolated from tumors and spleens on day 7, and the percentage of reporter-positive $CD8^{+}V\alpha2^{+}V\beta5^{+}$ T cells was determined by flow cytometry. **b**, FACS analysis of T cell enrichment in tumors compared to spleen (as described above) for cells expressing a panel of Ppp2r2d or Cblb shRNAs (upper panels). Ppp2r2d and Cblb mRNA levels were measured by qPCR prior to T cell transfer (lower panels). The strongest T cell enrichment in tumors was observed for shRNAs with >80% knock-down efficiency at the mRNA level (shRNAs #1 and 2 for both Ppp2r2d and Cblb). **c**, Quantification of Ppp2r2d protein by tandem mass spectrometry. Cytokine pre-treated OT-I cells were transduced with LacZ or Ppp2r2d shRNAs and sorted to purity using the Thy1.1 marker gene. Isotopically labeled peptides (referred to as AQUA peptides) specific for Ppp2r2d and Actin B were synthesized for quantification. Cell lysates were separated by SDS-PAGE and tryptic peptides eluted from gel slices. AQUA peptides (300 fmol) were added to samples to enable quantification by LC-MS/MS. AQUA peptides co-eluted with endogenous Ppp2r2d and Actin B peptides from the LC column, yet had a 10 Da higher molecular weight than the endogenous peptides. Data are represented as the ratio of endogenous (end) to AQUA peptides for both Actin B and Ppp2r2d in T cells expressing Ppp2r2d or LacZ shRNAs. Statistical significance was examined with Graphpad 6.0 software using the Student *t*-test (* $p = 0.0062$).

Supplementary Figure 4 □ Specificity of Ppp2r2d shRNA. a, Generation of mutant Ppp2r2d cDNA with wild-type protein sequence but disrupted shRNA binding site. Both mutant and wild-type Ppp2r2d

cDNAs were cloned into a modified pLKO.3G vector with a 2A peptide ribosomal skip sequence and GFP. This approach resulted in stoichiometric expression of Ppp2r2d protein and GFP in EL4 thymoma cells. GFP-expressing EL4 cells were sorted to purity and transduced with LacZ or Ppp2r2d shRNA vectors expressing a Thy1.1 reporter. shRNA-transduced ($Thy1.1^+$) cells were analyzed by flow cytometry for GFP expression. The Ppp2r2d shRNA reduced GFP levels when wild-type Ppp2r2d cDNA, but not when mutant Ppp2r2d cDNA was co-expressed. **b**, Expression of Ppp2r2d mutant cDNA prevents phenotype induced by Ppp2r2d shRNA. OT-I T cells were transduced with a vector encoding LacZ shRNA, Ppp2r2d shRNA or Ppp2r2d shRNA plus mutant Ppp2r2d cDNA. The different cell populations were normalized for transduction efficiency and co-injected into B16-Ova tumor bearing mice. The percentage of each T cell population in tumors and spleens was quantified by gating on $CD8^+V\alpha2^+V\beta5^+$ T cells; transduced cells were detected based on expression of Thy1.1 or Ametrine/GFP fluorescent reporters (representative data from 2 independent experiments, n=3 mice per experiment). **c**, Real-time PCR analysis for Ppp2r2d expression in OT-I T cells transduced with LacZ shRNA, Ppp2r2d shRNA, and Ppp2r2d shRNA plus Ppp2r2d mutant cDNA.

Supplementary Figure 5 □ Expression profiles of gene-silenced CD8 T cells in tumors. OT-I T cells were transduced with lentiviral vectors driving expression of one of five experimental shRNAs or LacZ control shRNA. T cells were injected into day 14 B16-Ova tumor-bearing mice and isolated from tumors and spleens 7 days later. Cells were sorted to high purity and total RNA was obtained for Affymetrix gene expression profiling. For each shRNA arrays were performed in triplicate (6 mice per group). **a**, Two genes (Egr2 and Ptpn2) have known functions in T cells. Enrichment in tumor versus spleen was calculated based on deep sequencing results from the secondary screen. **b**, Clustering of mean expression levels for mRNAs found to be significantly regulated by T cells in spleens or tumors

expressing the LacZ control shRNA or one of five experimental shRNAs. Significant expression differences were defined as an Anova *p* value ≤0.01 between T cells expressing LacZ control shRNA or one of five experimental shRNAs (Alk, Arhgap5, Egr2, Ptpn2 or Ppp2r2d) (JMP-Genomics 6.0, SAS Institute Inc.). mRNAs significantly regulated in one or more treatment groups are shown after clustering (Fast Ward). **c**, Venn diagram showing overlaps between expression signatures by tumor-infiltrating T cells transduced with one of the five experimental shRNAs (signatures defined as an Anova $p \leq 0.01$ as described above). Indicated are the numbers of overlapping probe IDs for any combination of the 5 signatures, as indicated by the overlapping ovals. The significance of the overlaps versus that expected by random chance (Fishers Exact Test) is shown in the accompanying table.

Supplementary Figure 6 □ Ppp2r2d shRNA enhances T cell proliferation and reduces apoptosis. **a**, Proliferation of Ppp2r2d shRNA-expressing T cells in tumors and tumor-draining lymph nodes. OT-I T cells expressing Ppp2r2d or LacZ shRNAs were labeled with CFSE and injected into B16-Ova tumor-bearing mice. T cells were isolated from the indicated organs on days 1, 3, 5 and 7 to examine the extent of T cell proliferation based on dilution of the CSFE dye. T cells that had not diluted CFSE (non-dividing cells) were quantified (right). **b,** Viability of tumor-infiltrating T cells. OT-I T cells expressing Pp2r2d or LacZ shRNAs were injected into B16-Ova tumor-bearing mice. T cells were isolated on day 7 and apoptosis was assessed by intracellular staining with an antibody specific for activated caspase-3. **c,** OT-I T cells expressing LacZ or Ppp2r2d shRNAs were labeled with CFSE and stimulated with B16-Ova tumor cells for 72 h. Cells were then stained with anti-CD8 and annexin V and analyzed by flow cytometry. Data for all experiments are representative of two independent trials (n=3; * $p \leq 0.05$, ** $p \leq 0.01$, Student's *t*-test). Error bars denote standard deviation.

Supplementary Figure 7 □ Cytokine secretion by gene-silenced tumor-infiltrating T cells. a, Intracellular cytokine staining for IFNγ by LacZ and Ppp2r2d shRNA-expressing T cells harvested from B16-Ova tumors (primary flow cytometry analysis for data summarized in Figure 3d). **b-d,** Ex vivo analysis of cytokine production by tumor-infiltrating T cells at a single-cell level using a nanowell device. LacZ or Ppp2r2d shRNA-expressing OT-I cells were injected into mice bearing day 14 B16-Ova tumors. After 7 days, GFP^+ (shRNA-expressing) OT-I T cells were sorted from tumors by FACS and deposited into a nanowell device modified with supported lipid bilayers presenting anti-CD3/CD28. The device contained a total of 84,672 wells of picoliter volume. T cells were activated for 3h (CD3/CD28 antibodies on bilayers), followed by placement of a slide with immobilized cytokine capture antibodies on the device (microengraving) for a 1h period (total stimulation time of 4h). Slides were then removed and stained with secondary fluorophore-conjugated cytokine antibodies prior to analysis in a microarray reader. **b,** Representative examples of single cells in nanowells and corresponding patterns of cytokine secretion revealed by microengraving**.** Cells in nanowells were labeled with SYTOX green (dead cell marker) and a plasma membrane dye to identify live cells. **c,** Bar graph showing percentage of LacZ or Ppp2r2d shRNA-expressing OT-I T cells secreting the indicated cytokines and cytokine combinations. **d,** Cytokine secretion rates. Data from standard calibration curves were used to calculate secretion rates for each cell. The horizontal black lines represent the mean and standard deviation. Statistical significance was tested using the Mann Whitney test (* $p<0.05$).

Supplementary Figure 8 □ Phenotypic characterization using memory, activation and exhaustion markers. a, The majority of adoptively transferred OT-I cells have a memory phenotype in lymph nodes but an effector phenotype in tumors. Cytokine pre-treated cells were transduced with Ppp2r2d or

LacZ shRNAs and injected into mice bearing 14 day B16-Ova tumors. On day 7, T cells were harvested from the indicated organs and stained with CD62L and CD44 antibodies. FACS analysis of shRNA-expressing OT-I cells was performed by gating on CD8/Thy1.1 double-positive cells. **b,** Analysis of exhaustion markers. OT-I cells were harvested from draining lymph nodes and tumors of mice and stained with a antibodies specific for TIM-3, LAG-3, PD-1 and CD25. **c,** Intracellular staining for granzyme B by OT-I T cells in tumor-draining lymph nodes and tumors. For all experiments (n=3; * $p \leq 0.05$, ** $p \leq 0.01$, Student's *t*-test); error bars denote standard deviation.

Supplementary Figure 9 □ Histological characterization of anti-tumor response. a, Infiltration of shRNA-expressing T cells into tumors. OT-I T cells were transduced with LacZ or Ppp2r2d shRNA vectors encoding a GFP reporter and injected into B16-Ova tumor-bearing mice. After 7 days, tumors were carefully excised and frozen sections stained with anti-GFP and DAPI to enumerate shRNA-expressing OT-I T cells in tumors. **b,** Tumor cell apoptosis. TUNEL immunohistochemistry was performed on tissue sections and apoptotic cells were quantified. **c,** MHC class I expression by tumor cells. Tumors were excised from treated mice, digested with collagenase and stained with CD45.2 and H-2K^b antibodies. FACS analysis for H-2K^b was performed by gating on CD45.2-negative cells.

Supplementary Table 1. Results from primary and secondary screens. The Excel file lists gene name, gene ID, shRNA clone ID, targeting sequence and enrichment of shRNAs in tumors relative to spleen. The first tab shows results from primary screens, the second tab data from secondary screens.

Supplemental methods

Experimental animals. C57BL/6 mice, TRP-1 mice (transgenic mice expressing T-cell receptor (TCR) specific for tyrosinase-related protein 1)[22], pmel-1 mice (transgenic mice expressing TCR specific for gp100)[17], and *b2m*$^{-/-}$ mice[23] were purchased from The Jackson Laboratory. The Rag1$^{-/-}$ OT-I mice[15] were purchased from Taconic Farms, Inc. Female mice aged 7-10 weeks were used for experiments. Mice were bred at the Dana-Farber Cancer Institute animal facility. All experimental procedures were approved by the Dana-Farber Cancer Institute Animal Care and Use Committee.

Cell lines. EL4 thymoma[39] and B16-F10 melanoma[14] cells were purchased from ATCC and maintained in RPMI 1640 supplemented with 10% FBS, 2mM L-glutamine, 100μg/ml streptomycin and 100μg/ml penicillin. Ovalbumin-expressing B16 tumor cells (B16-Ova) were maintained in the same media with addition of 600μg/mL G418 (Invitrogen).

Vectors and shRNA sequences. pLKO.3G vector was obtained from The RNAi Consortium. pLKO-Thy1.1, pLKO-Ametrine, pLKO-RFP, pLKO-TFP vectors were modified from pLKO.3G vector by replacing GFP with the corresponding reporter gene. The 10 shRNA sequences for Ppp2r2d and Cblb are listed below in order of activity (highest to lowest, Fig. S3). The LacZ control shRNA sequence is also listed. All other shRNA sequences can be found in Supplementary Table 1.

#	Gene	Clone ID	Sequence
	LacZ	TRCN0000072227	GCGCTAATCACGACGCGCTGT
1	Ppp2r2d	TRCN0000080900	CCCACATCAGTGCAATGTATT
2	Ppp2r2d	ND000492	CCACAGTGGTCGATACATGAT
3	Ppp2r2d	TRCN0000431278	GAGAATTAACCTATGGCATTT
4	Ppp2r2d	ND000486	GCTCAATAAAGGCCATTACTC
5	Ppp2r2d	TRCN0000080901	CCATTTAGAATTACGGCACTA
6	Ppp2r2d	TRCN0000430828	ATAGTGATCATGAAACATATC
7	Ppp2r2d	TRCN0000080899	GCCACCAATAACTTGTATATA
8	Ppp2r2d	TRCN0000080902	CGGTTCAGACAGTGCCATTAT
9	Ppp2r2d	TRCN0000427220	TCATCTCCACCGTTGAGTTTA
10	Ppp2r2d	TRCN0000425449	ATGCTCATACATATCACATAA
1	Cblb	ND000025	CGAGCGATCCGGCTCTTTAAA
2	Cblb	ND000030	AGCCAGGTCCAATTCCATTTC
3	Cblb	TRCN0000244606	CCCTGATTTAACCGGATTATG
4	Cblb	ND000026	ATCGAACATCCCAGATTTAGG
5	Cblb	TRCN0000244603	CTACACCTCACGATCATATAA
6	Cblb	ND000024	TACACCTCACGATCATATAAA
7	Cblb	TRCN0000244605	TGAGCGAGAATGAGTACTTTA
8	Cblb	TRCN0000244604	CCAGATTTAGGCATCTATTTG
9	Cblb	TRCN0000244607	CTTGTACTCCAGTACCATAAT
10	Cblb	ND000027	TCTACATCGATAGTCTCATGA

Antibodies and flow cytometry. Single-cell suspensions were stained in PBS, 2% FBS with labeled antibodies at 4□°C for 20 minutes, followed by two washes with ice-cold PBS, 2% FBS. Cells were analyzed/sorted using a FACSAria (BD Biosciences) and FlowJo software (TriStar). Antibodies used were specific for CD4, CD8, Vα2, Vβ5.1/5.2, Thy1.1, CD25, CD44, CD62L, CD69, CD122, CD127, IFNγ, TNFα, PD-1, TIM-3, LAG-3, granzyme B, and H-2K^{b} (BioLegend), Vα3.2 (eBioscience), Vβ13, Vβ14 (BD Biosciences). Apoptotic cells were detected by labeling with annexin V (BioLegend) or activated caspase-3 antibody (Cell Signaling). Mouse anti-CD3/CD28 beads were purchased from Invitrogen.

Immunofluorescence and immunohistochemistry. B16-Ova tumors from mice treated with OT-I T cells expressing LacZ or Ppp2r2d shRNAs (GFP-expressing vector) were cryopreserved in optimal cutting temperature (O.C.T.) compound (Tissue-Tek). 10 μm-sections from cryopreserved tumors were were permeabilized with 0.2% Triton X-100, fixed in 4% paraformaldehyde and stained with a GFP antibody (Molecular Probes) in combination with DAPI. For TUNEL detection, sections were stained with TACS 2 TdT Blue Label (Trevigen) based on manufacturer's directions. Samples were visualized using a laser-scanning confocal microscope (Leica SP5X) and analyzed with ImageJ software (NIH).

qRT-PCR assay. Total RNA was extracted using TRIzol reagent (Invitrogen). RNA was reverse transcribed with the High Capacity cDNA Reverse Transcription kit (Applied Biosystems). Real time quantitative PCR reactions were performed in triplicates using an ABI 7900HT instrument with SYBR green (ABI). Rpl23 levels were used for normalization. The following primers were used: Ppp2r2d forward GGAAGCCGACATCATCTCCAC, Ppp2r2d reverse GTGAGCGCGGCCTTTATTCT; Cblb forward GGTCGCATTTTGGGGATTATTGA, Cblb reverse TTTGGCACAGTCTTACCACTTT; Rpl23 forward CTGTGAAGGGAATCAAGGGA and Rpl23 reverse TGTCGAATTACCACTGCTGG.

Quantification of Ppp2r2d protein levels by mass spectrometry. A previously reported approach for absolute quantification (AQUA) of proteins from cell lysates by mass spectrometry was used to measure the effect of Ppp2r2d shRNA expression at the protein level[40]. This strategy is based on a 'selective reaction monitoring' approach in which a synthetic peptide with incorporated stable isotopes is used as an internal standard for mass spectrometry analysis. OT-I cells expressing LacZ or Ppp2r2d shRNAs

were sorted to purity using FACS. Cells ($1x10^6$) were lysed in 1ml of MPER extraction reagent (Pierce) containing a Protease Inhibitor Cocktail (Sigma), 1mM EDTA and 1mM PMSF for 15 minutes on ice with occasional vortexing. Cell debris was removed by centrifugation and the protein supernatant was filtered (0.2µm SpinX centrifuge filter, Costar). Protein concentration was determined by Bradford assay (Biorad) and UV280 nm analysis (Nanodrop instrument); 0.1 mg of cellular proteins were separated by SDS-PAGE and stained with Coomassie blue reagent (Pierce). Gel bands corresponding to a MW range of 45-60kDa were excised followed by in-gel digestion of proteins with trypsin. Eluted peptides were spiked with 300 fmol of isotopically labeled Ppp2r2d (FFEEPEDPSS[13C-15N-R]-OH) and Actin B (GYSFTTTAE[13C-15N-R]-OH) peptides (21^{st} Century Biochemicals) for quantification by LC-MS/MS (LTQ XL Orbitrap, Thermo Scientific). The Ppp2r2d peptide was chosen from a region of the protein that differs from other regulatory subunits of PP2A. Initially, a LC-MS/MS run of a LacZ shRNA sample was analyzed to localize the Ppp2r2d and Actin B peptides that were being monitored. The AQUA peptides co-eluted with the corresponding endogenous peptides from the reverse-phase column, yet their higher MW (10 Da) enabled the ratio of peak intensity of endogenous and AQUA peptides to be determined using abundant peptide fragment ions. Triplicate samples were analyzed by SDS-PAGE - LC-MS/MS and statistical significance was determined using Graphpad Prism 6.0 software using a Student *t*-test (F test, * p=0.0062).

Microarray analysis. IL-7/IL-15 cultured OT-I T cells were transduced with one of five experimental shRNAs (Ppp2r2d, Arhgap5, Alk, Egr2, Ptpn2) or a LacZ control shRNA. Infected cells were sorted to purity using GFP encoded by the vector as a reporter. T cells (5×10^6) were injected i.v. into mice bearing day 14 B16-Ova tumors. Seven days later, shRNA-expressing OT-I T cells ($CD8^+GFP^+$) were isolated from tumors and spleens. Cells were sorted twice to high purity and total RNA was extracted

using TRIzol reagent (Invitrogen) for Affymetrix gene expression profiling (Mouse Genome 430 2.0 Arrays). Arrays for each shRNA were done in triplicate (6 mice per group).

Testing of on-target activity of Ppp2r2d shRNA. Wild-type Ppp2r2d cDNA was isolated by RT-PCR using forward primer 5' GGATCCATGGCAGGAGCTGGAGGC 3' and reverse primer: 5' GCTAGCATTAATTTTGTCCTGGAATATATACAAGTTATTGGTGG 3'. In this cDNA the target sequence of Ppp2r2d shRNA, CCCACATCAGTGCAATGTATT was mutated to TCCCCACCAATGTAACGTGTT by overlapping PCR (which conserves protein coding sequence) using forward primer: 5' TCCATCCCCACCAATGTAACGTGTTTGTTTACAGCAGCAGCAAGG 3' and reverse primer: 5' AAACAAACACGTTACATTGGTGGGGATGGAACTCTGCGGCAGTGA 3'. Both wild-type and mutant Ppp2r2d cDNAs were cloned into a modified pLKO.3 vector with a 2A ribosomal skip peptide-GFP sequence (resulting in stoichiometric Ppp2r2d and GFP expression in cells). Constructs were introduced into EL4 thymoma cells. GFP-expressing EL4 cells were sorted to purity and then transduced with LacZ or Ppp2r2d shRNA lentiviral vectors driving expression of a Thy1.1 reporter. shRNA-transduced ($Thy1.1^{+}$) cells were analyzed by flow cytometry for GFP expression. The Ppp2r2d shRNA was not able to reduce expression of the GFP reporter in cells expressing the mutant Ppp2r2d cDNA, demonstrating that the shRNA binding site had been successfully mutated.

Ppp2r2d shRNA was subsequently cloned into the mutant Ppp2r2d cDNA-2A-GFP construct which resulted in co-expression of Ppp2r2d shRNA and mutated Ppp2r2d cDNA in one vector. OT-I T cells were separately infected with lentiviruses encoding LacZ shRNA (Thy1.1), Ppp2r2d shRNA (Ametrine) or Ppp2r2d shRNA plus mutant Ppp2r2d cDNA (GFP). These three populations were then mixed at the same ratio and co-injected into mice bearing day 14 B16-Ova tumors. On day 7, each T cell population

was quantified in tumors and spleens by gating on OT-I ($V\alpha2^{+}V\beta5^{+}$) T cells followed by analysis of populations marked by Thy1.1, Ametrine or GFP expression.

Nanowell analysis of cytokine production at a single cell level

Materials. Antibodies used for T cell activation were anti-mouse CD3 (clone 145-2C11) and anti-mouse CD28 (clone 37.51) (Biolegend). Antibodies used to capture secreted cytokines were anti-mouse IFNγ (clone R4-6A2, Biolegend), anti-mouse IL-2 (clone JES6-1A12, Biolegend), anti-mouse TNFα (clone 6B8, Biolegend) and anti-mouse GM-CSF (clone MP1-22E9, Biolegend). Detection antibodies were anti-mouse IFNγ (clone XMG1.2, Biolegend), anti-mouse IL-2 (clone JES6-5H4, Biolegend), anti-mouse TNFα (clone MP6-XT22, Biolegend) and anti-mouse GM-CSF (clone MP1-31G6, Biolegend), and they were fluorescently labeled with appropriate Alexa Fluor dyes (Invitrogen) following manufacturer's instructions. The lipids used to prepare supported bilayers were: 1,2-dioleoyl-*sn*-glycero-3-phosphocholine (DOPC) and 1,2-dioleoyl-*sn*-glycero-3-phosphoethanolamine-*N*-(cap biotinyl) (Biotinyl Cap PE) (Avanti Polar Lipids).

Fabrication of PDMS arrays of nanowells and preparation of supported lipid bilayers. The array of nanowells was manufactured by injecting polydimethylsiloxane (PDMS, Dow Corning) prepared at a 10:1 base/catalyst weight ratio into a custom-built mold encasing a micropatterned silicon master. Arrays of nanowells were cured at 70 °C for 4-16 h. Each array comprised 72 x 24 blocks, each containing a 7 x 7 (50 μm x 50 μm x 50 μm) subarray of nanowells (total of 84,672 wells). The PDMS arrays adhered directly to a 3″ x 1″ glass slide forming a 1 mm thick layer. Supported lipid bilayers were prepared as described previously[41]. Bilayers were generated by applying DOPC liposomes

containing 2 mol% biotin-Cap-PE lipids on the PDMS array of nanowells. The surfaces were rinsed with deionized water to remove excess liposomes. Before use, the lipid bilayer was blocked with BSA in PBS (100 μg/mL) for 45 minutes. The bilayer was then incubated with 1 μg/mL of streptavidin in a solution of 100 μg/mL BSA in PBS, followed by incubation with biotinylated CD3 and CD28 antibodies. The device was rinsed extensively with PBS before adding the cells.

Microengraving. Capture antibodies were diluted in borate buffer (50 mM sodium borate, 8 mM sucrose, and 50 mM NaCl, pH 9.0) to a final concentration of 10 μg/mL and deposited on the surface of epoxy-modified slides for 1 h at room temperature. Slides were blocked with 3% non-fat milk in PBST (PBS with 0.05% (v/v) Tween 20) for 30 min at room temperature and washed with PBS before placing them into contact with the PDMS array of nanowells. A suspension of T cells was dispensed onto the surface of the nanowells, modified with a supported lipid bilayer in media and allowed to settle into the wells. The density of suspended cells applied to the array was optimized empirically to maximize well occupancy with single cells (typically ~30% of wells). After incubation of the cell-loaded wells, a glass slide coated with capture antibodies was then placed onto the loaded array for cytokine capture. The microarray and glass slide were held together by compression in a hybridization chamber (Agilent Technologies, G2534A) and incubated for 1h at 37 °C with 5% CO_2. The glass slide was then separated from the array and placed in PBS.

After microengraving, slides were incubated for 30 min with blocking buffer (PBS, 10mg/mL BSA, 0.05 % (v/v) Tween-20, 2% mouse serum and 2 mM sodium azide), washed with PBST (PBS+ 0.05% v/v Tween-20), and then incubated with fluorescence detection antibodies at 1 μg/mL for 45 min at 25°C. The slides were washed with PBST and PBS, rinsed briefly with water, and dried with a N_2 stream. Reference slides were generated at the end of each experiment with the same detection antibodies used on the printed slides. For reference slides, antibodies were diluted in water, spotted onto blank poly-L-

lysine slides (1 μL/spot), and the reference slides were dried under vacuum. Slides were scanned using a Genepix 4200AL microarray scanner (Molecular Devices). The median fluorescence intensity of each spot was extracted using Genepix Pro.

On-chip image-based cytometry. Before imaging, T cells were stained with CellMask™ Plasma Membrane Stain (Invitrogen, Life Technologies) and SYTOX green (for detection of dead cells, Life Technologies). The cell-loaded arrays of nanowells were mounted face-up on the microscope with a coverslip placed on top of the array. Images were acquired on an automated inverted epifluorescence microscope (Carl Zeiss). Transmitted light and epifluoresence micrographs were collected block-by-block (7 x 7 microwells per block). The resulting collection of images was analyzed using a custom program to determine the number of cells present in each well and the mean fluorescent intensity of each label. Only viable T cells were considered for the analysis. Although the cells expressed GFP, the fluorescent intensity of GFP was negligible under the utilized microscope acquisition setting compared to SYTOX green, enabling identification of dead cells.

Data analysis. Data extracted from both on-chip cytometry and printed cytokines were matched in Microsoft Excel using unique identifiers assigned to each well within the array. The dataset was filtered to include wells containing only single cells. To compensate from signal bleed-through and convert the measured fluorescence intensity for the captured cytokines from a given cell into a rate of secretion, the data from standard calibration curves (from reference slides) prepared with known amounts of detection antibodies was used to convert measured intensities to a number of molecules, as described previously [42].

39. Gorer, P.A. Studies in antibody response of mice to tumour inoculation. *Br J Cancer* **4**, 372-379 (1950).
40. Gerber, S.A., Rush, J., Stemman, O., Kirschner, M.W. & Gygi, S.P. Absolute quantification of proteins and phosphoproteins from cell lysates by tandem MS. *Proceedings of the National Academy of Sciences of the United States of America* **100**, 6940-6945 (2003).
41. Torres, A.J., Contento, R.L., Gordo, S., Wucherpfennig, K.W. & Love, J.C. Functional single-cell analysis of T-cell activation by supported lipid bilayer-tethered ligands on arrays of nanowells. *Lab Chip* **13**, 90-99 (2013).
42. Han, Q., Bradshaw, E.M., Nilsson, B., Hafler, D.A. & Love, J.C. Multidimensional analysis of the frequencies and rates of cytokine secretion from single cells by quantitative microengraving. *Lab Chip* **10**, 1391-1400 (2010).

Figure 1

a

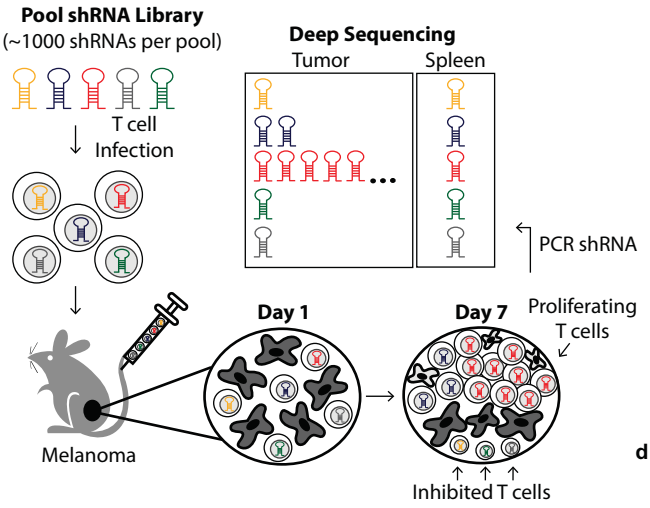

b

		T cell Dysfunction	Kinase/ Phosphatase	shRNA Enrichment
1° Screen	Genes	255	1307	4-10x: 123
	shRNAs	1275	6535	10-20x: 17
	Candidate Genes	32	82	> 20x: 1
2° Screen	Genes	32	43	4-10x: 191
	shRNAs	480	645	10-20x: 27
	Candidate Genes	17	26	> 20x: 1

c

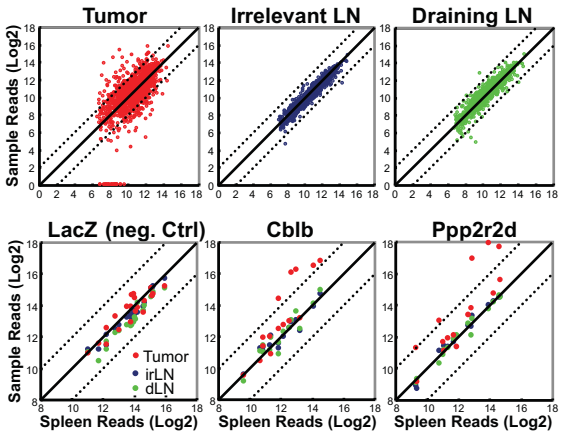

d

Function	Genes
Inhibition of TCR signaling	Cblb, Dgka, Dgkz, Fyn, Inpp5b, Ppp3cc, Ptpn2, Stk17b, Tnk1
Phosphoinositol metabolism	Dgka, Dgkz, Impk, Inpp5b, Sbf1
Inhibitory cytokine signaling pathways	Smad2, Socs1, Socs3
AMP signaling, inhibition of mTOR	Entpd1, Prkab2, Nuak
Cell cycle	Cdkn2a, Pkd1, Ppp2r2d
Actin and microtubules	Arhgap5, Mast2, Rock1
Potential nuclear functions	Blvrb, Egr2, Impk, Jun, Ppm1g
Role in cancer cells	Alk, Arhgap5, Eif2ak3, Hipk1, Met, Nuak, Pdzk1ip1, Rock1, Yes1

Figure 2

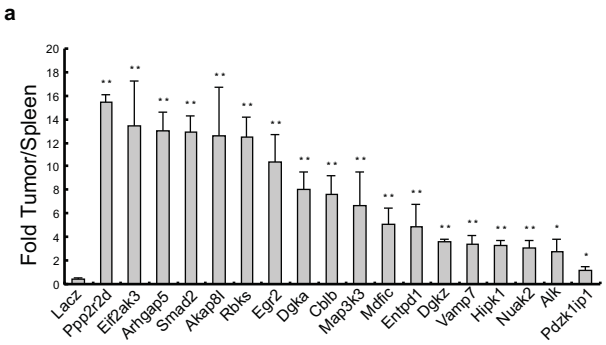
a
Fold Tumor/Spleen
Lacz
Ppp2r2d
Eif2ak3
Arhgap5
Smad2
Akap8l
Rbks
Egr2
Dgka
Cblb
Map3k3
Mdfic
Entpd1
Dgkz
Vamp7
Hipk1
Nuak2
Alk
Pdzk1ip1

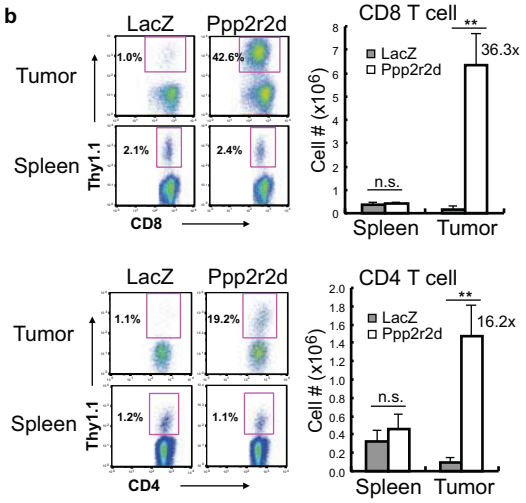
b
LacZ
Ppp2r2d
Tumor
Spleen
Thy1.1
CD8
1.0%
42.6%
2.1%
2.4%
CD8 T cell
Cell # (x10^6)
LacZ
Ppp2r2d
36.3x
n.s.
Spleen
Tumor
CD4
1.1%
19.2%
1.2%
1.1%
CD4 T cell
16.2x

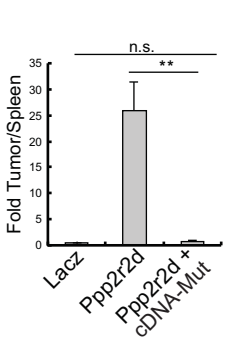
c
Fold Tumor/Spleen
n.s.
Lacz
Ppp2r2d
Ppp2r2d + cDNA-Mut

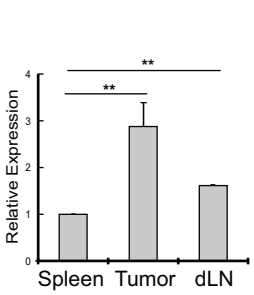
d
Relative Expression
Spleen
Tumor
dLN

Figure 3

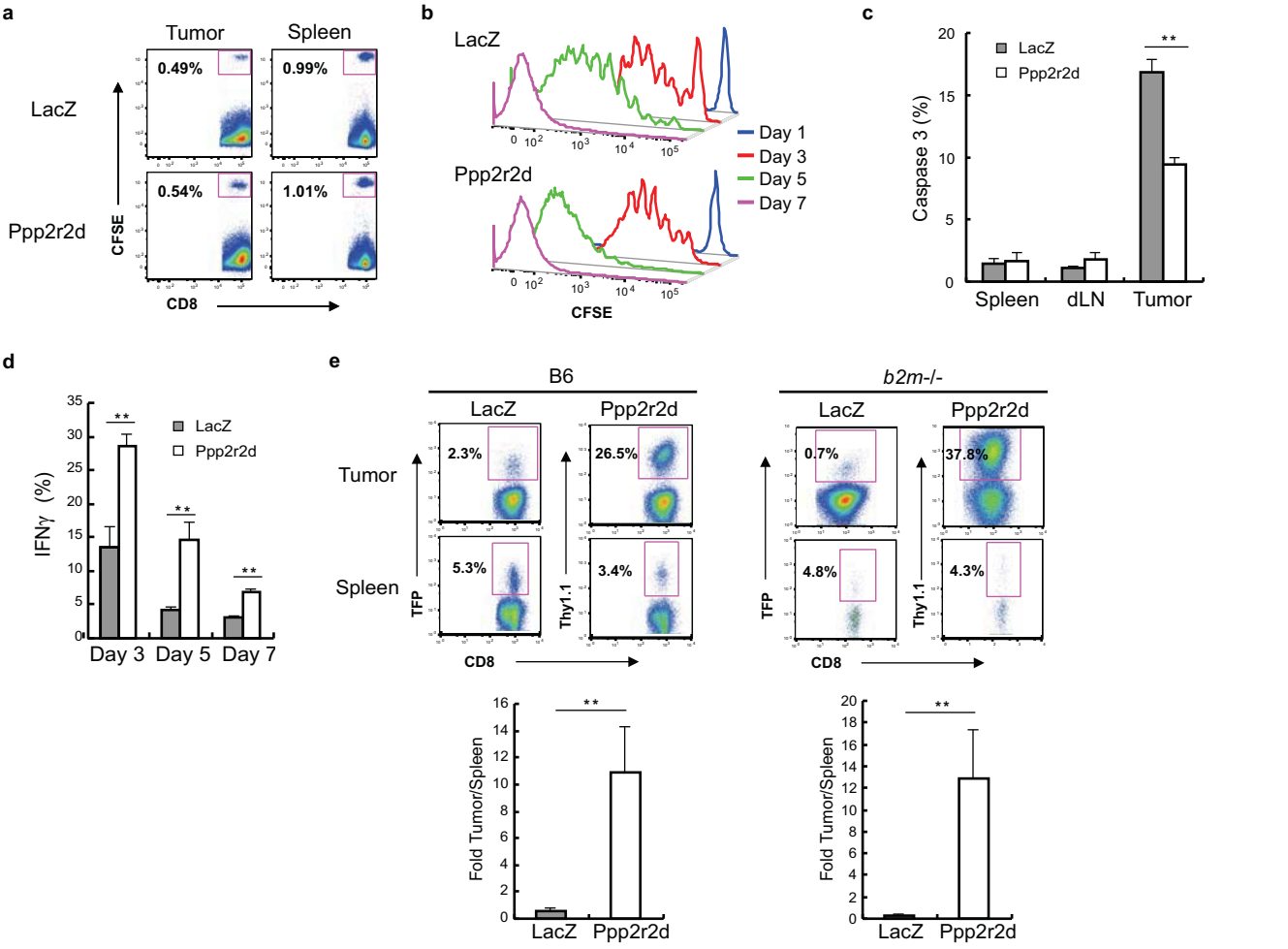
a
Tumor
Spleen
LacZ
Ppp2r2d
0.49%
0.99%
0.54%
1.01%
CFSE
CD8
b
LacZ
Ppp2r2d
Day 1
Day 3
Day 5
Day 7
CFSE
c
LacZ
Ppp2r2d
Caspase 3 (%)
Spleen
dLN
Tumor
d
LacZ
Ppp2r2d
IFNγ (%)
Day 3
Day 5
Day 7
e
B6
b2m-/-
LacZ
Ppp2r2d
Tumor
Spleen
2.3%
26.5%
5.3%
3.4%
0.7%
37.8%
4.8%
4.3%
TFP
Thy1.1
CD8
Fold Tumor/Spleen

Figure 4

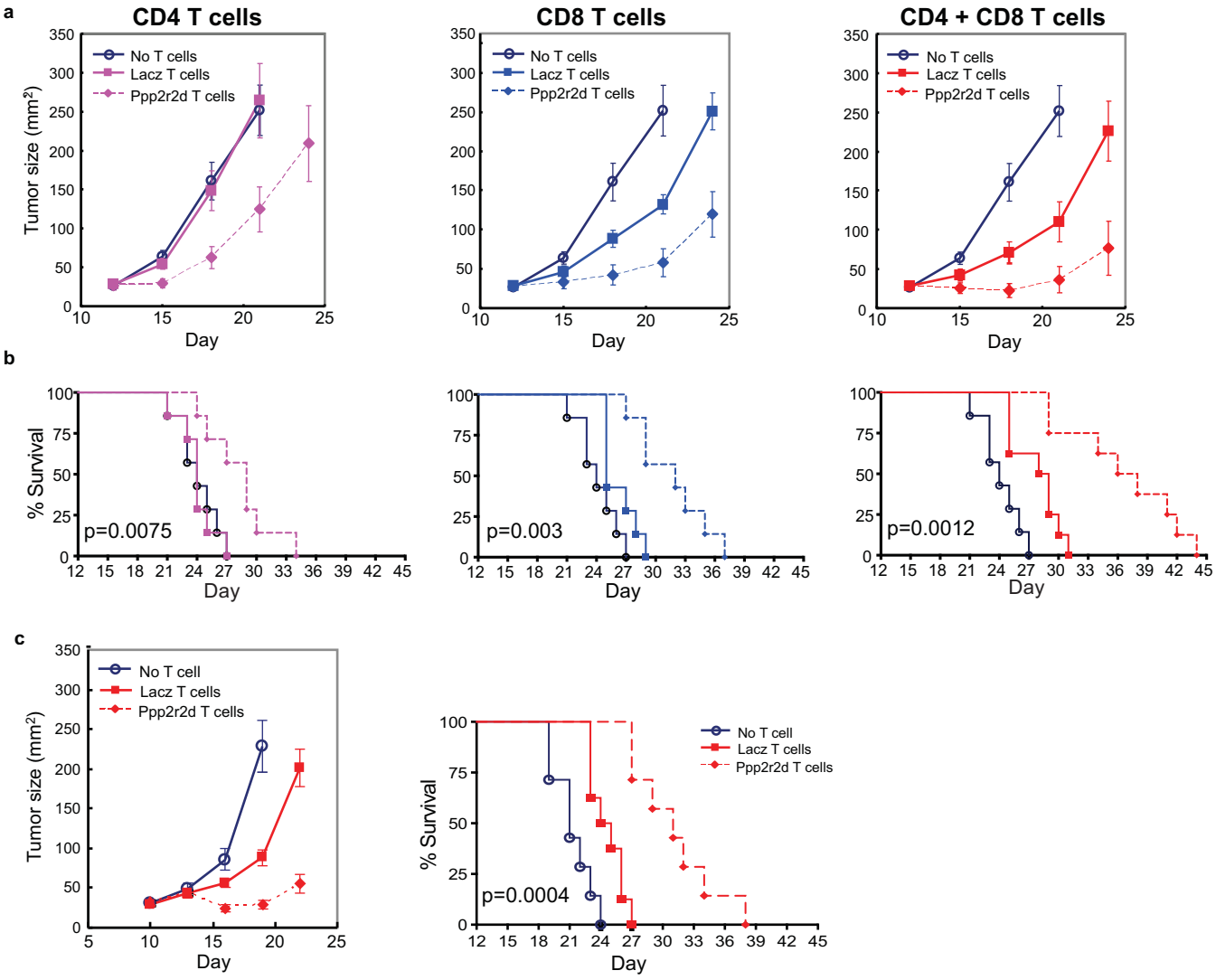
a
CD4 T cells
CD8 T cells
CD4 + CD8 T cells
No T cells
Lacz T cells
Ppp2r2d T cells
Tumor size (mm²)
Day
b
% Survival
p=0.0075
p=0.003
p=0.0012
Day
c
No T cell
Lacz T cells
Ppp2r2d T cells
Tumor size (mm²)
Day
% Survival
p=0.0004
Day

S. 1

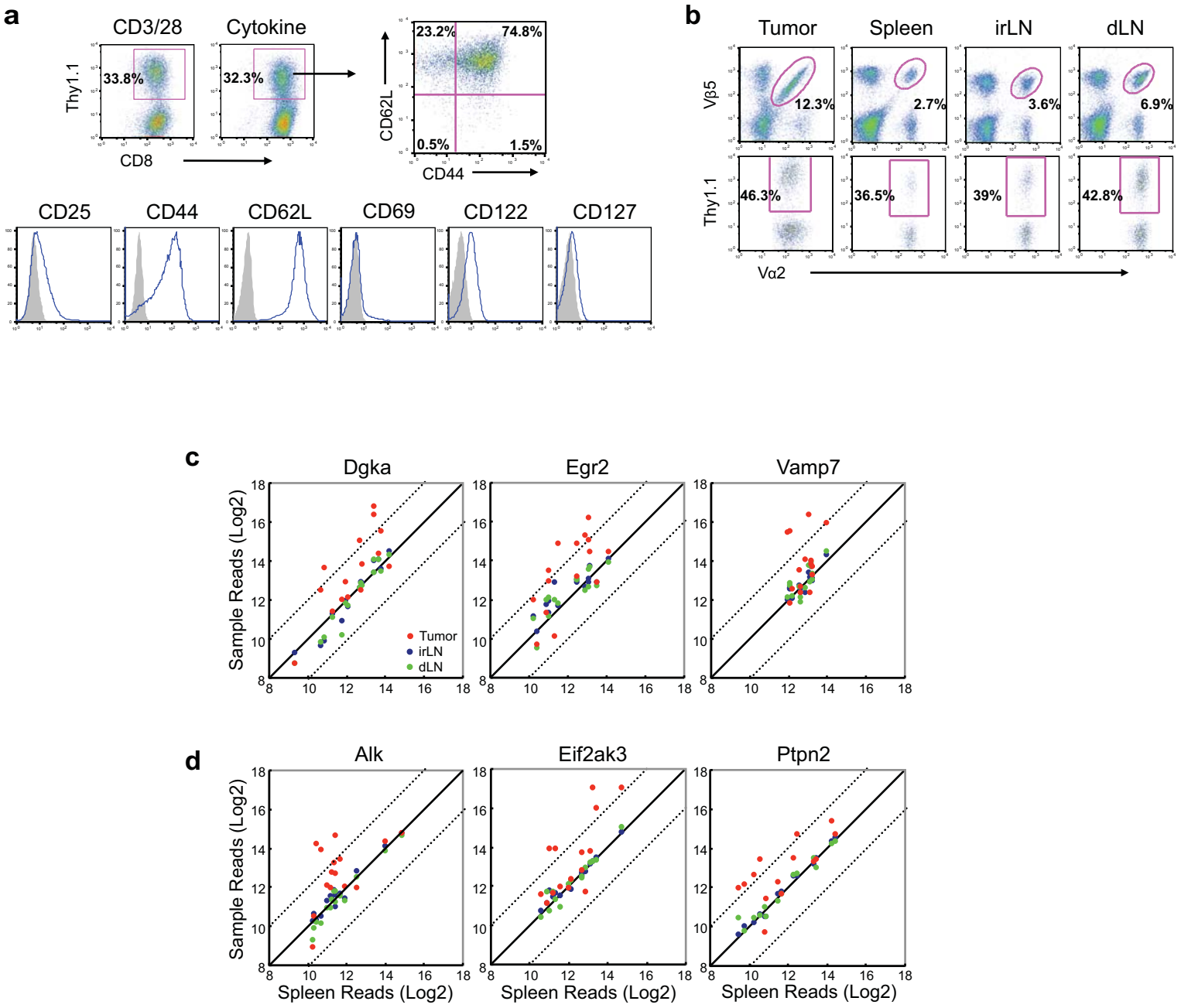
a
CD3/28
Cytokine
Thy1.1
33.8%
32.3%
CD8
CD62L
CD44
23.2%
74.8%
0.5%
1.5%
CD25
CD44
CD62L
CD69
CD122
CD127
b
Tumor
Spleen
irLN
dLN
Vβ5
12.3%
2.7%
3.6%
6.9%
Thy1.1
46.3%
36.5%
39%
42.8%
Vα2
c
Dgka
Egr2
Vamp7
Sample Reads (Log2)
Tumor
irLN
dLN
d
Alk
Eif2ak3
Ptpn2
Sample Reads (Log2)
Spleen Reads (Log2)

S. 2

a

	Symbol	Total # shRNAs	Enrichment (fold)	Function
1	**Dgkz**	6	5.2 - 14.0	Phosphorylates and thereby inactivates DAG
2	**Egr2**	6	4.0 - 10.2	Transcription factor involved in T cell unresponsiveness, expression of Cblb
3	**Smad2**	5	6.7 - 30.3	TGF beta signaling pathway
4	**Cblb**	5	4.1 - 10.8	E3 ubiquitin ligase (degradation of TCR and signaling molecules; ko mice reject tumors)
5	**Inpp5b**	5	4.3 - 9.5	Inositol polyphosphate-5-phosphatase, hydrolyzes PIP2
6	**Socs1**	5	4.1 - 8.5	Inhibitor of cytokine signaling
7	**Jun**	5	5.2 - 6.4	Persistent AP-1 activation in tumor-infiltrating T cells leads to upregulated PD-1
8	**Vamp7**	4	4.0 - 11.3	Vesicle associated transmembrane protein
9	**Dgka**	4	5.0 - 10.2	Phosphorylates and thereby inactivates DAG
10	**Mdfic**	4	4.4 - 10.0	Inhibits viral gene expression, interacts with cyclin T1 and T2
11	**Nptxr**	4	4.0 - 7.2	Pentraxin Receptor
12	**Socs3**	4	4.6 - 6.3	Inhibitor of cytokine signaling
13	**Entpd1**	3	6.5 - 13.3	Extracellular degradation of ATP to AMP (an inhibitory signal through AMP kinase)
14	**Pdz1ip1**	3	4.8 - 12.9	Pdzk1 interacting protein, expression correlates with tumor progression
15	**F11r**	3	4.6 - 6.8	Cell Migration
16	**Fyn**	3	4.1 - 6.5	Inhibits activation of resting T cells (through Csk)
17	**Ypel2**	3	4.6 - 5.1	Function unknown

b

	Symbol	Total # shRNAs	Enrichment (fold)	Function
1	**Rbks**	6	4.0 - 12.8	Ribokinase, carbohydrate metabolism
2	**Pkd1**	6	4.9 - 9.9	Cell cycle arrest (activates JAK/STAT pathway)
3	**Ppp2r2d**	5	4.0 - 17.2	Regulatory subunit of PP2A phosphatase
4	**Eif2ak3**	5	4.8 - 13.4	ER stress sensor, resistance of cancer cells to chemotherapy
5	**Ptpn2**	5	4.7 - 7.4	Inhibitor of T cell and cytokine signaling
6	**Hipk1**	4	4.5 - 12.3	Interacts with p53 and c-myb, knockout mice develop fewer carcinogen-induced tumors
7	**Grk6**	4	4.2 - 11	Regulator of particular G-protein coupled receptors
8	**Cdkn2a**	4	4.1 - 7.2	G1 cell cycle arrest and apoptosis in T cells
9	**Sbf1**	4	4.8 - 6.9	Activates MTMR2, which dephosphorylates PI(3)P and PI(3,5)P2
10	**Ipmk**	4	4.0 - 6.9	Inositol polyphosphate kinase, nuclear functions such as chromatin remodeling
11	**Rock1**	4	4.1 - 6.5	Rho kinase, inhibitors have shown activity in mouse models of cancer
12	**Stk17b**	4	4.0 - 6.4	Inhibitor of T cell signaling forms complex with protein kinase D
13	**Mast2**	4	4.1 - 5.1	Microtubule-associated serine/threonine kinase
14	**Arhgap5**	3	6.0 - 15.7	Negative regulator of Rho GTPases, inhibition can reduce cancer cell invasion
15	**Alk**	3	9.6 - 13.5	Anaplastic lymphoma kinase (translocation of nucleophosmin and ALK in ALCL)
16	**Nuak**	3	4.5 - 13.1	Member of AMP-activated protein kinase-related kinase family, oncogene in melanoma
17	**Akap8l**	3	4.4 - 11.8	A-kinase anchoring protein, recruits cAMP-dependent protein kinase (PKA) to chromatin
18	**Pdp1**	3	4.1 - 9.8	Pyruvate dehydrogenase phosphatase 1, regulation of glucose metabolism
19	**Yes1**	3	5.4 - 9.7	Src family kinase, oncogene in several tumors
20	**Met**	3	4.1 - 8.9	Receptor tyrosine kinase, involved in hepatocellular and other cancers
21	**Ppm1g**	3	6.2 - 8.2	Dephosphorylates spliceosome substrates and histones H2A-H2B
22	**Blvrb**	3	5.3 - 8.0	Biliverdin reductase, also transcription factor, arrest of cell cycle
23	**Tnk1**	3	5.2 - 7.6	Downregulates Ras pathway (phosphorylation of Grb2), inhibition of NF-kB pathway
24	**Prkab2**	3	4.1 - 7.0	Subunit of AMP kinase, inhibits fatty acid synthesis and mTOR pathway
25	**Trpm7**	3	4.9 - 5.9	Ion channel and serine-threonine kinase
26	**Ppp3cc**	3	4.2 - 4.4	Regulatory subunit of calcineurin (phosphatase in T cell receptor signaling)

S. 3

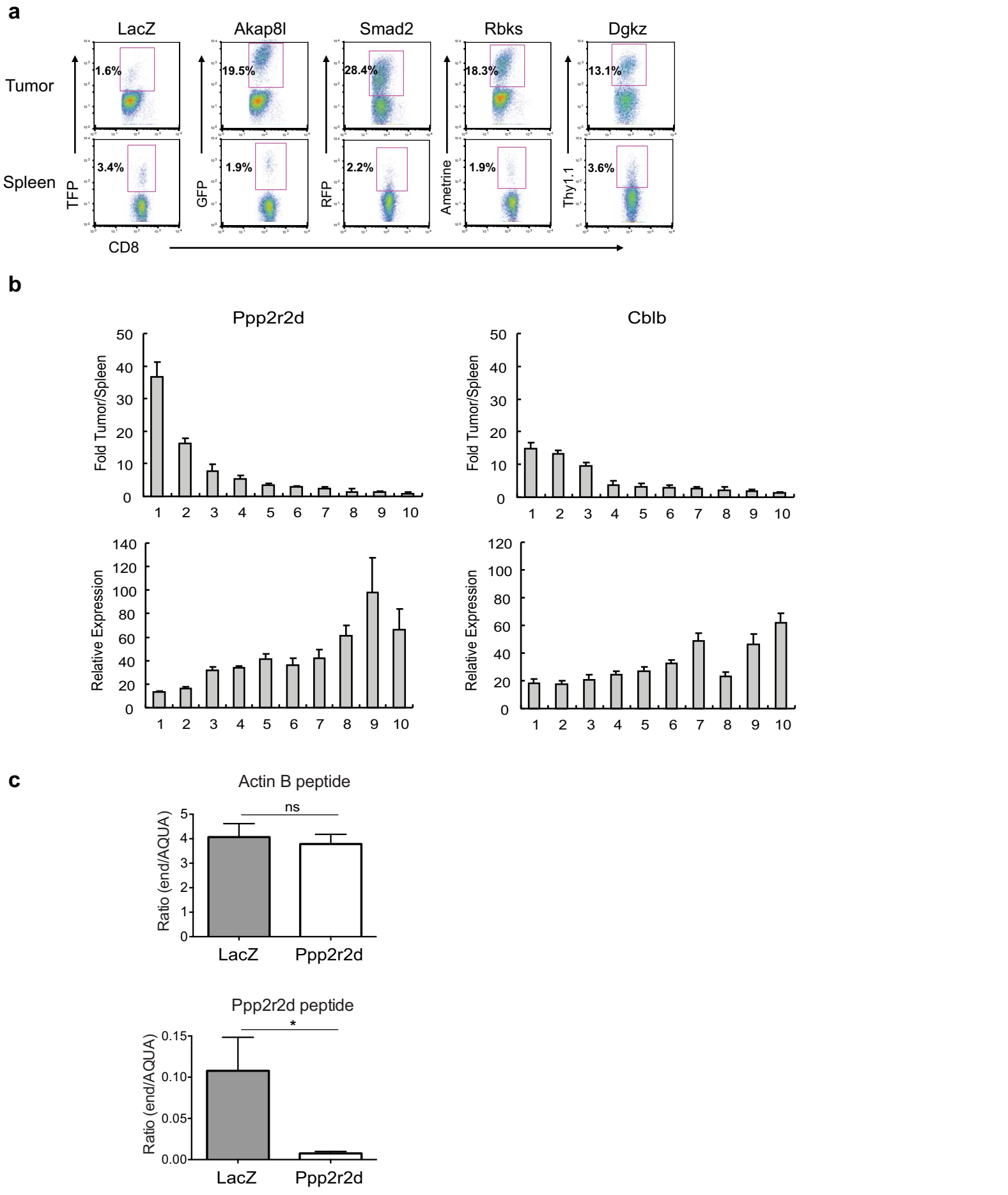
a
LacZ
Akap8l
Smad2
Rbks
Dgkz
Tumor
Spleen
1.6%
19.5%
28.4%
18.3%
13.1%
3.4%
1.9%
2.2%
1.9%
3.6%
TFP
GFP
RFP
Ametrine
Thy1.1
CD8
b
Ppp2r2d
CbIb
Fold Tumor/Spleen
Relative Expression
c
Actin B peptide
ns
Ratio (end/AQUA)
LacZ
Ppp2r2d
Ppp2r2d peptide
*

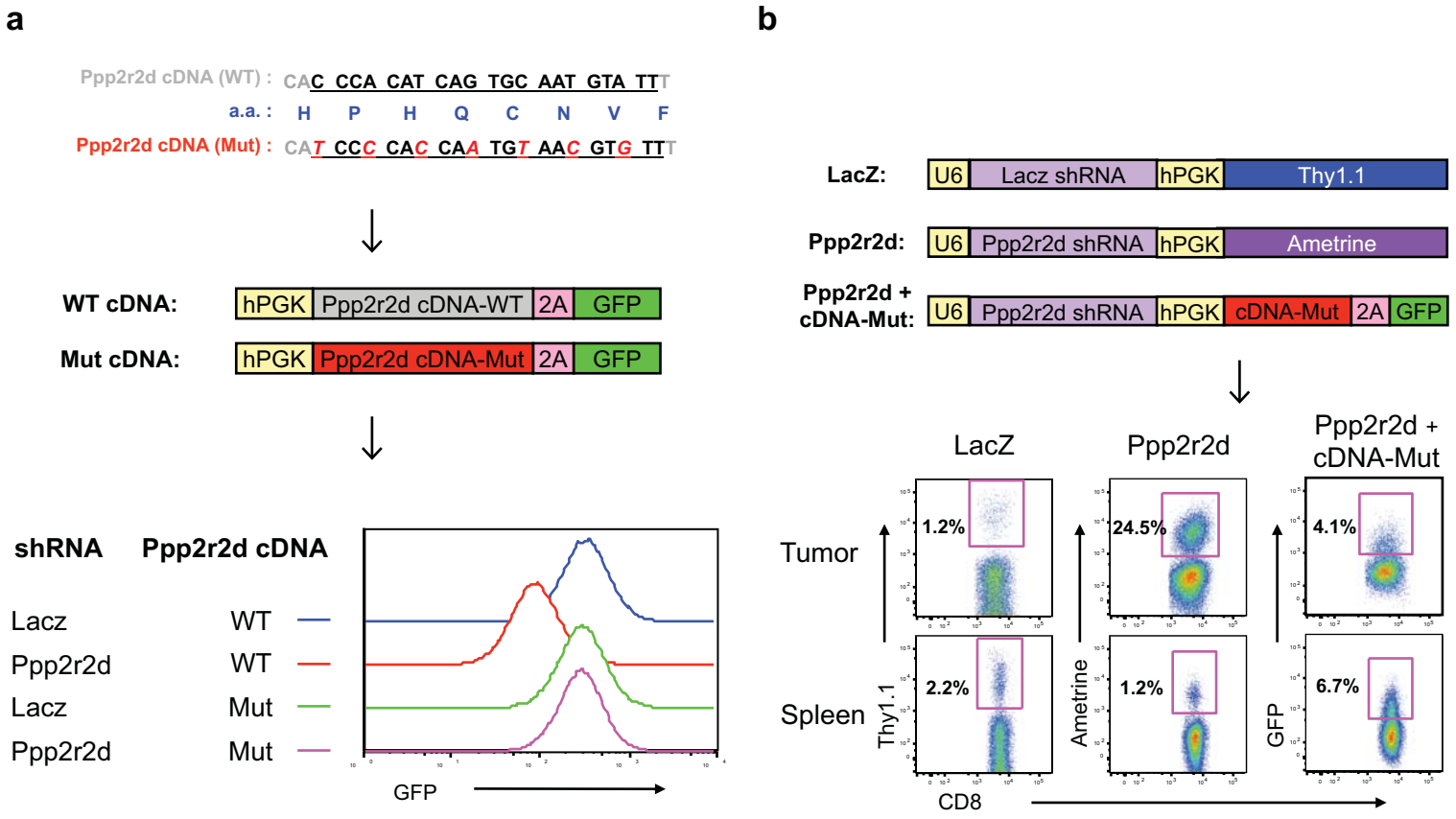
a
Ppp2r2d cDNA (WT) : CAC CCA CAT CAG TGC AAT GTA TTT
a.a. : H P H Q C N V F
Ppp2r2d cDNA (Mut) : CAT CCC CAC CAA TGT AAC GTG TTT
WT cDNA:
hPGK
Ppp2r2d cDNA-WT
2A
GFP
Mut cDNA:
hPGK
Ppp2r2d cDNA-Mut
2A
GFP
shRNA
Ppp2r2d cDNA
Lacz
WT
Ppp2r2d
WT
Lacz
Mut
Ppp2r2d
Mut
GFP
b
LacZ:
U6
Lacz shRNA
hPGK
Thy1.1
Ppp2r2d:
U6
Ppp2r2d shRNA
hPGK
Ametrine
Ppp2r2d + cDNA-Mut:
U6
Ppp2r2d shRNA
hPGK
cDNA-Mut
2A
GFP
LacZ
Ppp2r2d
Ppp2r2d + cDNA-Mut
Tumor
Spleen
1.2%
24.5%
4.1%
2.2%
1.2%
6.7%
Thy1.1
Ametrine
GFP
CD8

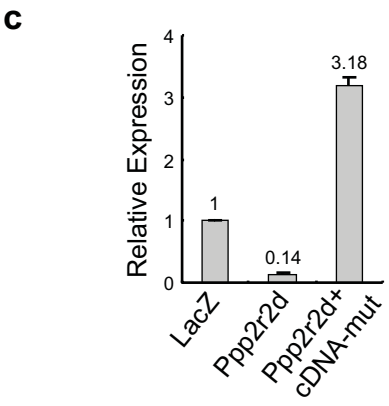
c
Relative Expression
0
1
2
3
4
1
0.14
3.18
LacZ
Ppp2r2d
Ppp2r2d+ cDNA-mut

S. 5

a

Gene Symbol	Function	Enrichment Fold
Ppp2r2d	Regulatory subunit of PP2A phosphatase	17.2
Arhgap5	Negative regulator of Rho GTPases	15.7
Alk	Anaplastic lymphoma kinase (translocation of nucleophosmin and ALK in ALCL)	13.5
Egr2	Transcription factor involved in T cell unresponsiveness, expression of Cblb	10.2
Ptpn2	Inhibitor of T cell and cytokine signaling	7.4

b

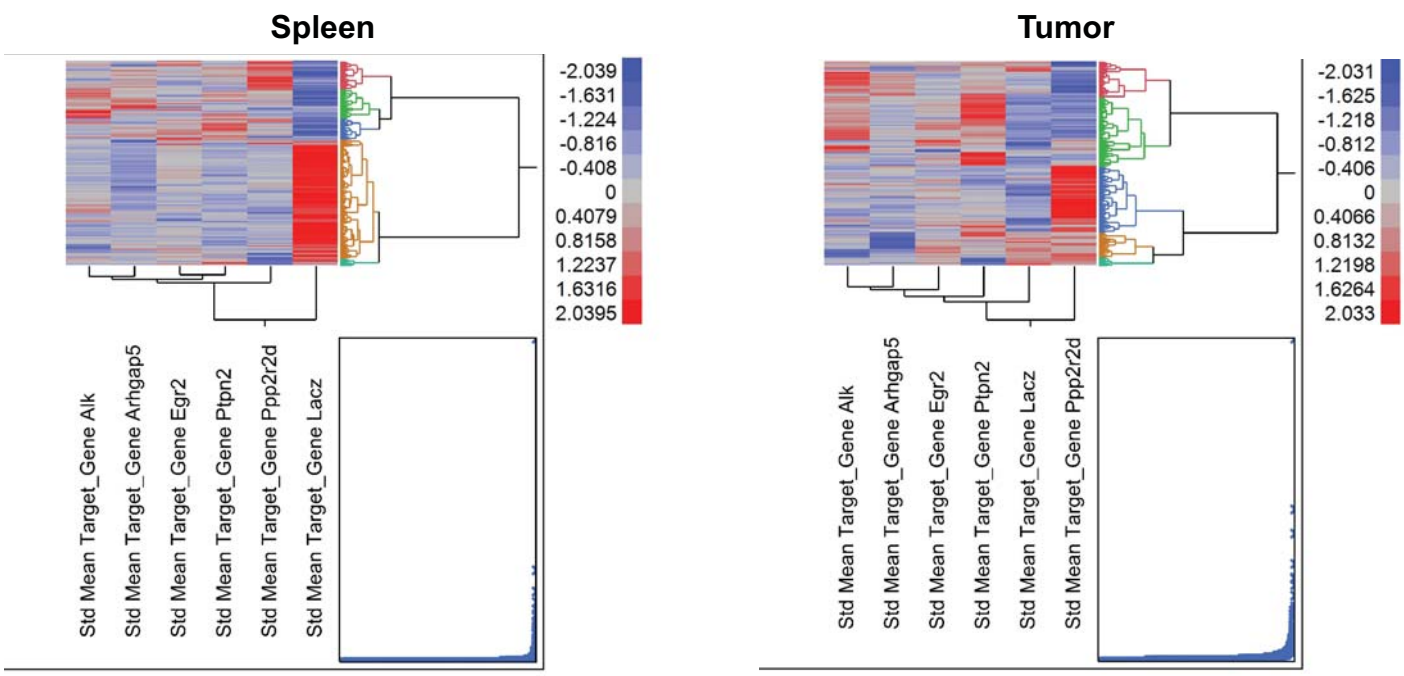

c

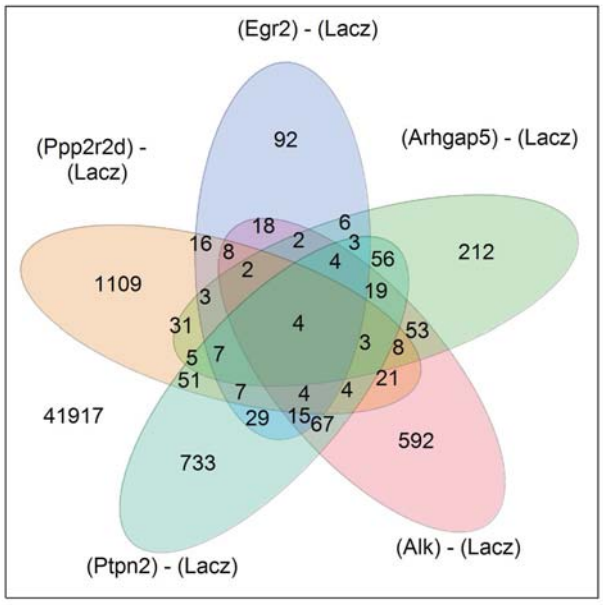

	Alk	Arhgap5	Egr2	Ppp2r2d	Ptpn2
Alk		1.0E-31	5.6E-14	ns	1.9E-23
Arhgap5			7.8E-07	9.5E-14	3.5E-16
Egr2				3.2E-08	3.3E-24
Ppp2r2d					1.6E-07
Ptpn2					

S. 6

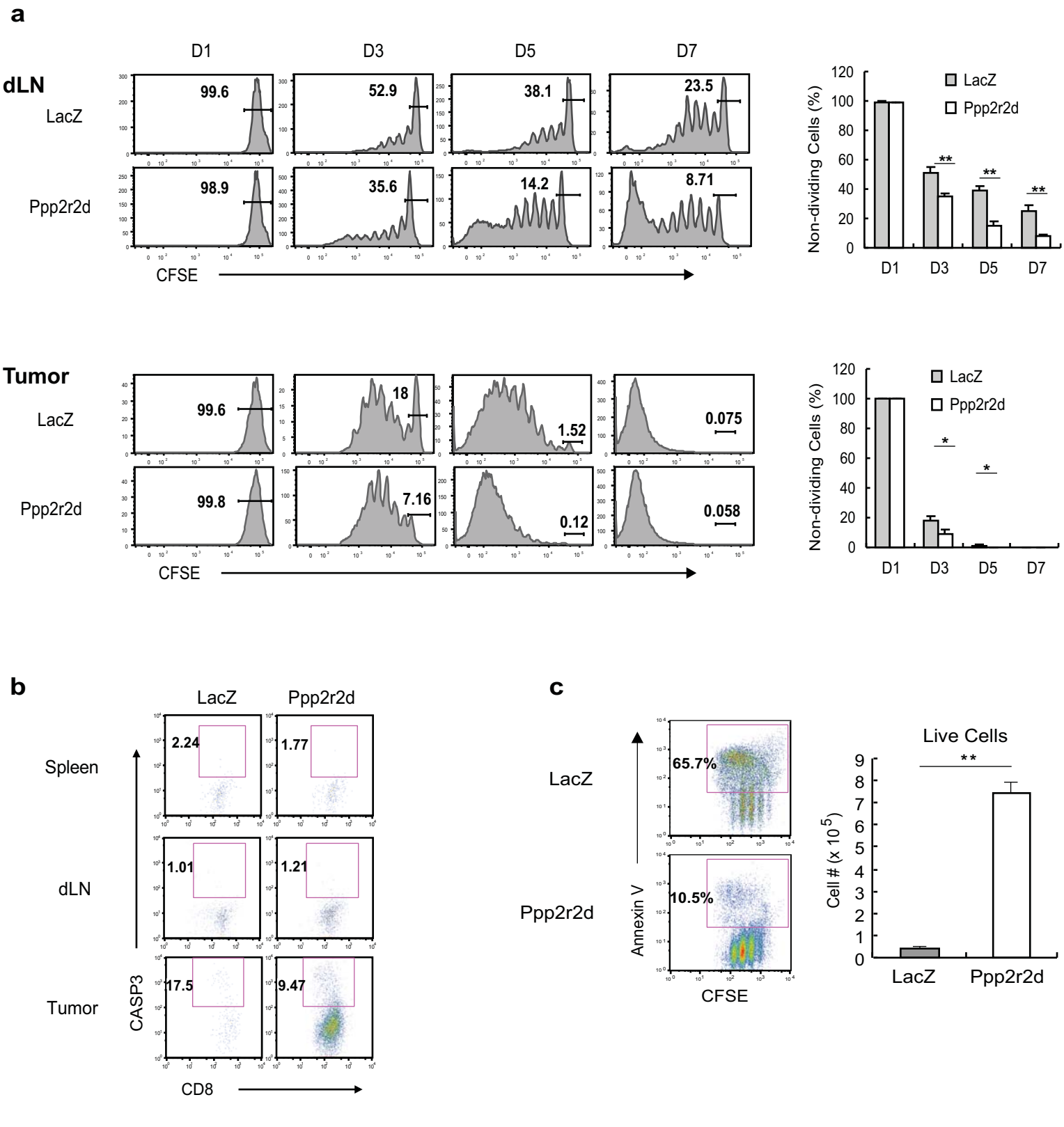
a
D1
D3
D5
D7
dLN
LacZ
Ppp2r2d
99.6
52.9
38.1
23.5
98.9
35.6
14.2
8.71
CFSE
Non-dividing Cells (%)
LacZ
Ppp2r2d
**
Tumor
99.6
18
1.52
0.075
99.8
7.16
0.12
0.058
*
b
LacZ
Ppp2r2d
Spleen
dLN
Tumor
2.24
1.77
1.01
1.21
17.5
9.47
CASP3
CD8
c
65.7%
10.5%
Annexin V
CFSE
Live Cells
Cell # (x 10^5)

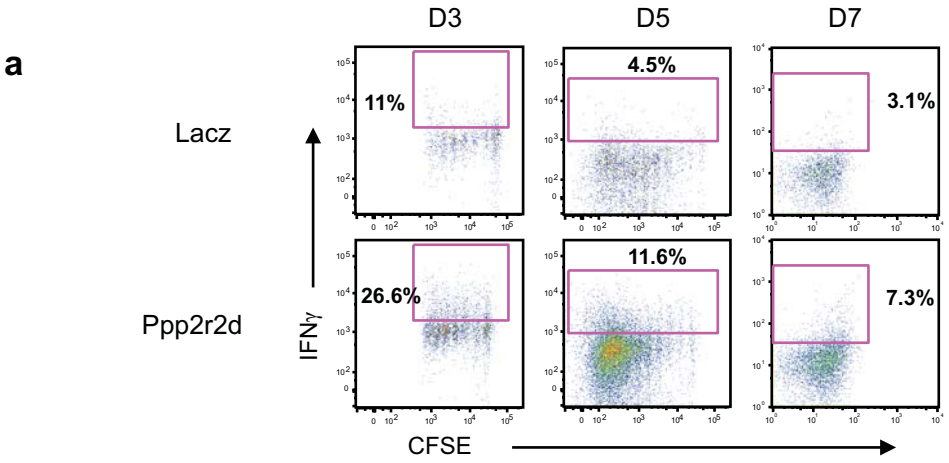
a
D3
D5
D7
Lacz
Ppp2r2d
11%
4.5%
3.1%
26.6%
11.6%
7.3%
IFNγ
CFSE

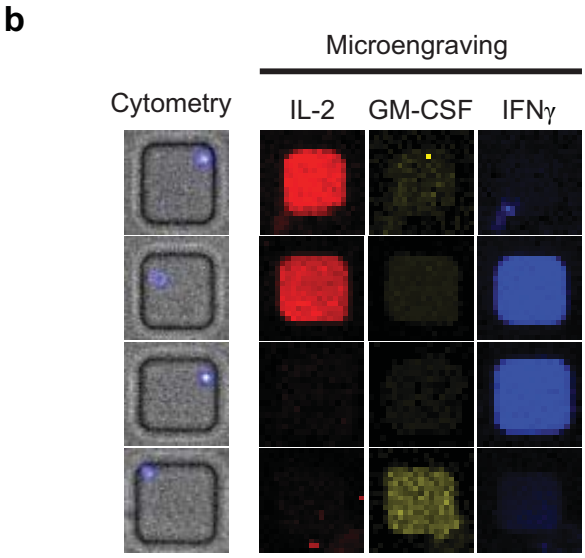
b
Microengraving
Cytometry
IL-2
GM-CSF
IFNγ

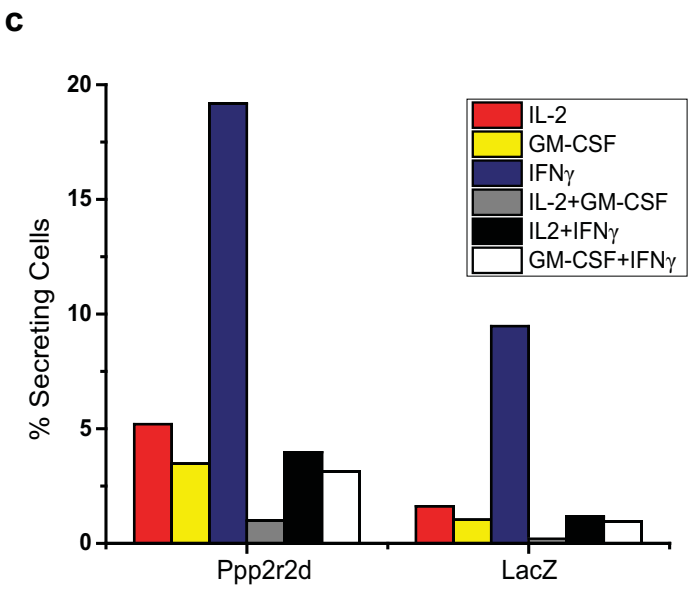
c
% Secreting Cells
20
15
10
5
0
IL-2
GM-CSF
IFNγ
IL-2+GM-CSF
IL2+IFNγ
GM-CSF+IFNγ
Ppp2r2d
LacZ

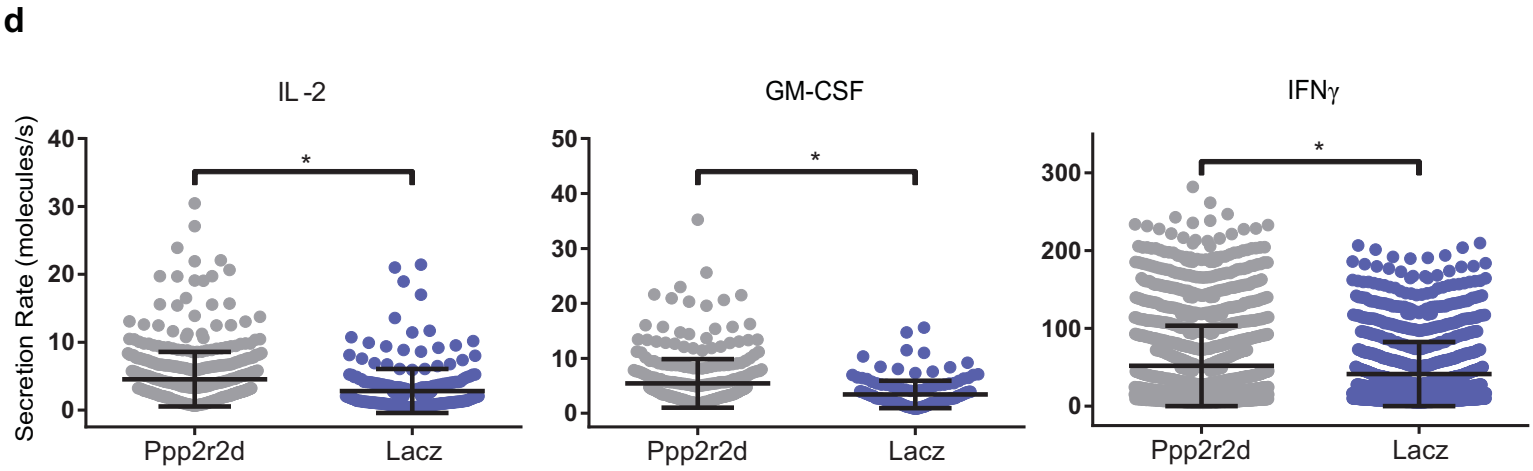
d
IL-2
GM-CSF
IFNγ
Secretion Rate (molecules/s)
40
30
20
10
0
50
300
200
100
*
Ppp2r2d
Lacz

S. 8

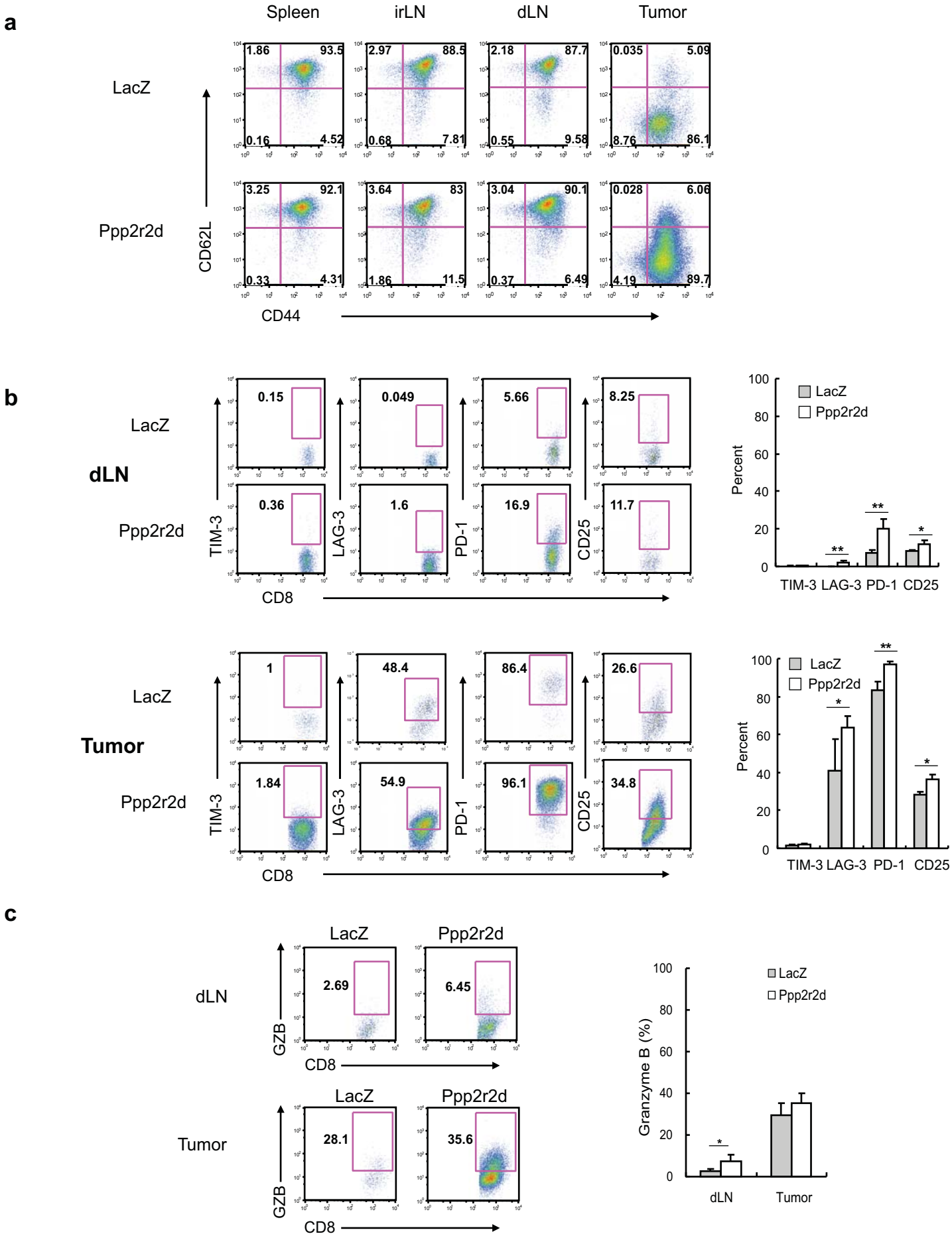
a
Spleen
irLN
dLN
Tumor
LacZ
Ppp2r2d
CD62L
CD44
1.86
93.5
0.16
4.52
2.97
88.5
0.68
7.81
2.18
87.7
0.55
9.58
0.035
5.09
8.76
86.1
3.25
92.1
0.33
4.31
3.64
83
1.86
11.5
3.04
90.1
0.37
6.49
0.028
6.06
4.19
89.7
b
dLN
Tumor
LacZ
Ppp2r2d
TIM-3
LAG-3
PD-1
CD25
CD8
0.15
0.049
5.66
8.25
0.36
1.6
16.9
11.7
1
48.4
86.4
26.6
1.84
54.9
96.1
34.8
Percent
TIM-3 LAG-3 PD-1 CD25
c
dLN
Tumor
GZB
CD8
2.69
6.45
28.1
35.6
Granzyme B (%)
dLN
Tumor

a

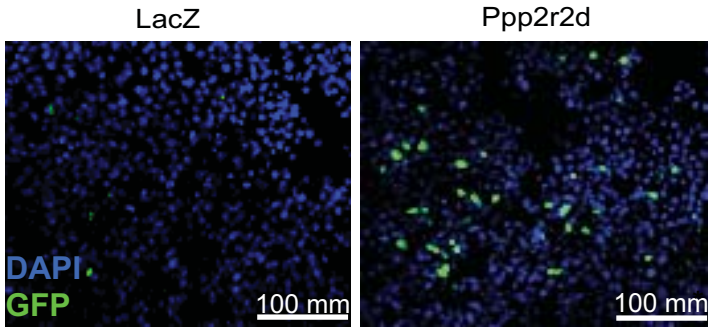
LacZ
Ppp2r2d
DAPI
GFP
100 mm
100 mm

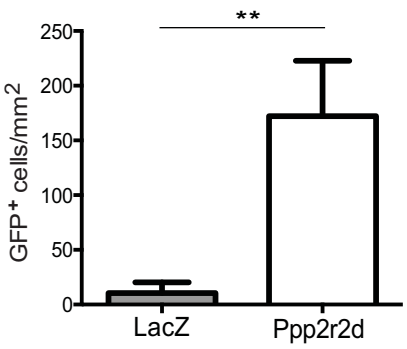
**
GFP+ cells/mm2
250
200
150
100
50
0
LacZ
Ppp2r2d

b

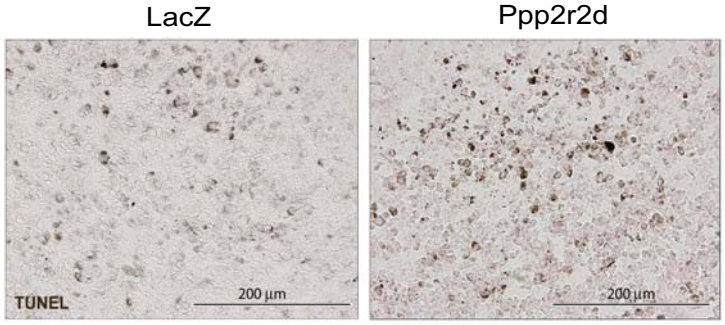
LacZ
Ppp2r2d
TUNEL
200 µm
200 µm

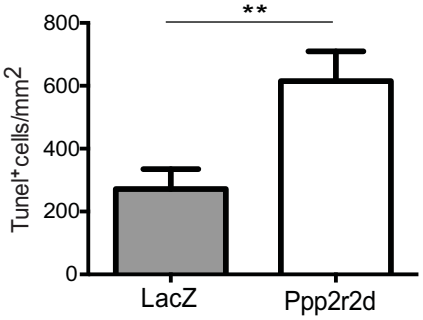
**
Tunel+cells/mm2
800
600
400
200
0
LacZ
Ppp2r2d

c

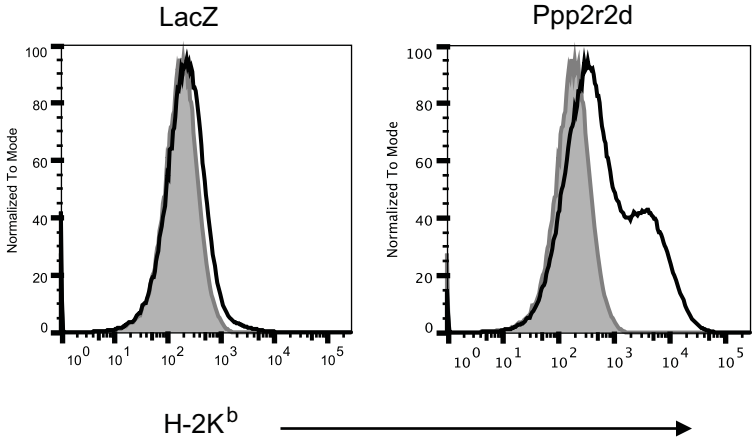
LacZ
Ppp2r2d
Normalized To Mode
Normalized To Mode
H-2Kb

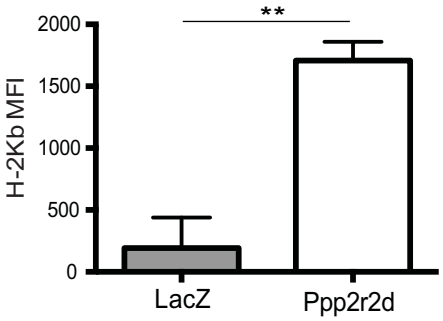
**
H-2Kb MFI
2000
1500
1000
500
0
LacZ
Ppp2r2d